Seismotectonics of the Explorer region

Jochen Braunmiller[1] and John Nábělek

College of Oceanic and Atmospheric Sciences, Oregon State University, Corvallis, Oregon, USA

Received 19 September 2001; revised 15 January 2002; accepted 20 January 2002; published 2 October 2002.

[1] The Explorer region offshore western Canada is a tectonically complex area surrounded by the Pacific, North America, and Juan de Fuca plates. Existing tectonic models for the region differ fundamentally. Proposed plate configurations range from multiple independent plate fragments to an Explorer plate now fused to North America along the continental margin and cut by Pacific–North America transform faults in the west. We present new seismological data constraining the region's current tectonics. We use three-component regional waveforms to determine the source parameters of 84 earthquakes with magnitude greater than 4. Combined with 34 Harvard centroid moment tensor solutions, they represent the region's largest earthquake source parameter data set obtained by robust waveform modeling techniques. In addition, we perform joint epicenter determination to relocate larger earthquakes recorded since 1918. The source parameters and improved locations provide a consistent tectonic picture. Earthquake slip vector azimuths along the Pacific plate boundary change smoothly and are significantly less northerly oriented than the Pacific-North America plate motion direction, requiring an independent Explorer plate. The present-day Pacific-Explorer boundary is formed by transform faults subparallel to the Revere-Dellwood-Wilson fault. Plate motion vectors indicate that the Winona block is part of the Explorer plate. Current Explorer motion is more northerly than indicated by magnetic anomalies prior to 2 Ma, implying a recent change, possibly coinciding with a northwestward ridge jump near Explorer plate's northern end transferring the Winona block from the Pacific to the Explorer plate. In response to these plate motion changes the region north of the western Sovanco fracture zone was assimilated into the Pacific plate. The region around the eastern Sovanco fracture zone, characterized by broadly distributed seismicity, is composed of well-defined sets of conjugate faults bounding rotating crustal blocks. Earthquake fault strikes agree with the dominant northwest-southeast fault sets; however, the conjugate sets must be also active to fully accommodate present-day Explorer plate motion. The SW portion of the strike-slip Nootka fault zone, the Explorer-Juan de Fuca plate boundary, is well defined by focused seismicity; however, its full extent under Nootka Island remains unresolved. The Explorer–North America boundary shows sporadic low-magnitude seismicity. Our Explorer–North America rotation pole predicts convergence varying from negligible at the boundary's northwest end to ~2 cm/yr at the SE end. This convergence can be accommodated either by subduction or by crustal thickening extending to the North American continent. We favor subduction based on low deformation rates observed by onshore GPS sites. The present Explorer plate system configuration is a result of stepwise reorientation of the Explorer ridge system, each step successively reducing the subduction rate relative to North America. *INDEX TERMS:* 7215 Seismology: Earthquake parameters; 7230 Seismology: Seismicity and seismotectonics; 8158 Tectonophysics: Evolution of the Earth: Plate motions—present and recent (3040); 3040 Marine Geology and Geophysics: Plate tectonics (8150, 8155, 8157, 8158); *KEYWORDS:* seismotectonics, Explorer plate, microplates, regional moment tensors, earthquake source parameters, seismicity

Citation: Braunmiller J., and J. Nábělek, Seismotectonics of the Explorer region, *J. Geophys. Res.*, *107*(B10), 2208, doi:10.1029/2001JB000220, 2002.

1. Introduction

[2] The Explorer region, offshore western Canada, is a small remnant of the Farallon plate that occupied large parts of the northeast Pacific basin in Cretaceous times. Two contradictory models exist for the region's current tectonics. According to the first, the region forms the independent

[1]Now at Swiss Seismological Service, ETH-Hönggerberg, Zurich, Switzerland.

0148-0227/02/2001JB000220$09.00

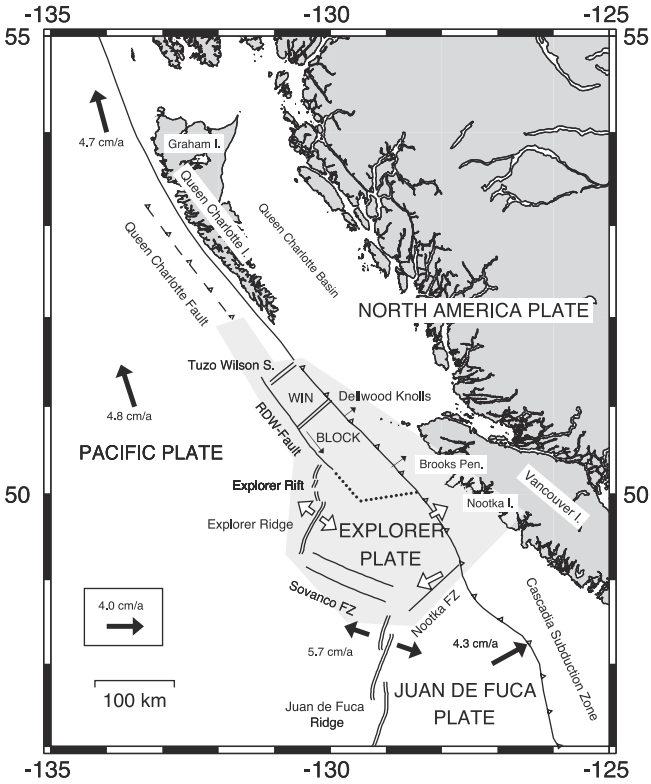

Figure 1. Map of Explorer region and surroundings. Plate boundaries are based on *Riddihough*'s [1984] and *Davis and Riddihough*'s [1982] tectonic models. Solid lines are active plate boundaries (single lines are transform faults, double lines are spreading centers, barbed lines are subduction zones with barbs in downgoing plate direction). The wide double line outlines the width of the Sovanco fracture zone, and the dots sketch the Explorer-Winona boundary. Plate motion vectors (solid arrows) are from NUVEL-1A [*DeMets et al.*, 1994] for Pacific-North America motion and from *Wilson* [1993] for Pacific-Juan de Fuca and Juan de Fuca-North America motion. Open arrows are Explorer relative plate motions averaged over last 1 Myr [*Riddihough*, 1984] (in text, we refer to these most recent magnetically determined plate motions as the "Riddihough model"). Winona block motions (thin arrows), described only qualitatively by *Davis and Riddihough* [1982], are not to scale. Abbreviations are RDW for Revere-Dellwood-Wilson, Win for Winona, FZ for fault zone, I for island, S for seamount, Pen for peninsula.

Explorer plate [*Riddihough*, 1977, 1984] surrounded by the Pacific, North America, and Juan de Fuca plates (Figure 1). The second model (Figure 2), in contrast, has the region cut by a transform fault forming the Pacific-North America plate boundary, with Explorer plate's remnants now permanently attached to either side [*Barr and Chase*, 1974; *Rohr and Furlong*, 1995]. This controversy raised our interest, and we present new, previously unavailable, seismological data to constrain current regional plate motions.

[3] Since the Tertiary, the Farallon plate and its successors have steadily decreased in size and experienced multiple stages of plate breakup [*Engebretson et al.*, 1985; *Lonsdale*, 1991; *Stock and Lee*, 1994]. The first major breakup, into the Juan de Fuca plate in the north and the Nazca-Cocos plate in the south, occurred about 55–50 Ma when the Farallon-Pacific spreading center approached the Farallon-North America subduction zone [*Stock and Molnar*, 1988; *Atwater*, 1989]. Juan de Fuca plate's size has steadily decreased since its inception due to northward migration of its southern triple junction [*Atwater*, 1989] and additional plate fragmentation. For the last few million years, two fragments, the Gorda deformation zone [*Riddihough*, 1980; *Wilson*, 1986, 1989] in the south and the Explorer plate [*Barr and Chase*, 1974; *Riddihough*, 1977, 1984; *Botros and Johnson*, 1988] in the north, moved distinctly from the remainder of the Juan de Fuca plate.

[4] A difference between Explorer and Juan de Fuca ridge orientation, starting about 4 Ma, requires an independent Explorer plate at least since that time [*Riddihough*,

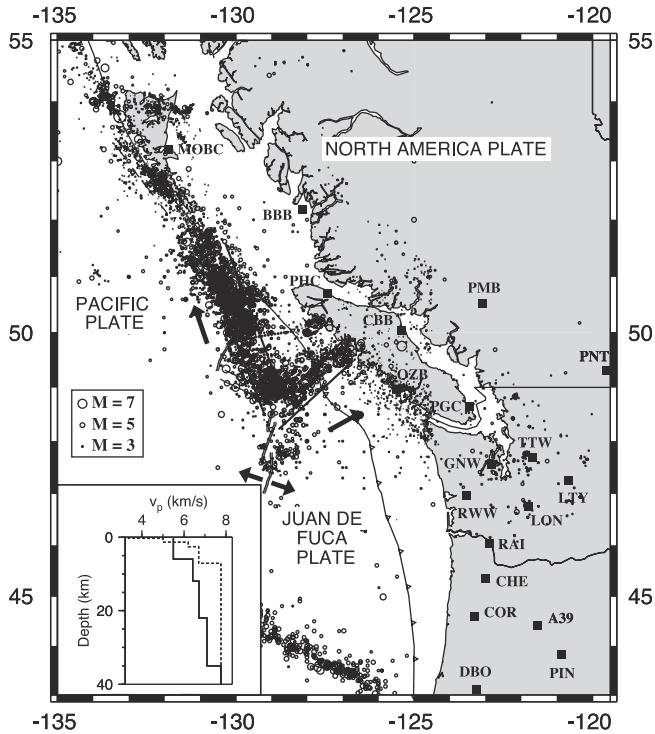

Figure 2. Map of broadband seismic stations (solid squares) and 1912–1997 seismicity (open circles; from the International Seismological Centre, Preliminary Determination of Epicenters, Geological Survey of Canada and Decade of North American Geophysics catalogs). A northwest trending, broad epicenter band inside Explorer region parallels the predicted Pacific-North America motion direction (solid arrow). A northeast trending band marks Nootka fault zone. Parallel lines indicate the tectonic model of *Barr and Chase* [1974] and *Rohr and Furlong* [1995]. The activity along the Explorer-North America boundary is low. Not shown are stations NEW and WALA east and DLBC north of the map. The inset shows the *P* wave velocity-depth model used for synthetic seismogram calculations. We applied an oceanic model (dashed line) for stations MOBC, BBB, PHC, and OZB, and a land model (solid line) for all other stations. The v_p/v_s ratio used is 1.78 except for the thin uppermost sediment layer in the oceanic model where the ratio was set to 1.91.

1984; *Botros and Johnson*, 1988]. Explorer region's tectonics complicated further 1–2 Myr ago when spreading shifted from offshore Brooks peninsula to the vicinity of the Dellwood Knolls and Tuzo Wilson seamounts [*Riddihough et al.*, 1980]. The Revere-Dellwood-Wilson transform fault's more northerly orientation compared to Explorer ridge's spreading direction led *Davis and Riddihough* [1982] to suggested that the Winona block (Figure 1) is an independent plate fragment. Figure 1 depicts the current plate boundaries and expected plate motions in the Explorer region following *Riddihough* [1984] and *Davis and Riddihough* [1982]. The model includes two small, independent plates: Explorer plate and Winona block. An entirely different model for Explorer region's current plate motions was presented by *Barr and Chase* [1974] and *Rohr and Furlong* [1995]. They argue that seismicity, which appears to cut in a northwesterly direction through the Explorer region (Figure 2), defines a new Pacific-North America transform plate boundary. This second model implies that independent motion of the small Explorer and Winona plate fragments ceased before they were entirely subducted beneath North America. Similar ''plate capture'' is documented for several microplates in the seafloor magnetic anomaly record offshore California and Baja California [*Lonsdale*, 1991]. Each of these preserved microplates fragmented off the southward retreating Cocos plate and moved as an independent plate for only a few million years before becoming attached to the Pacific plate [*Atwater*, 1989; *Lonsdale*, 1991; *Stock and Lee*, 1994].

[5] The purpose of our study is to determine the Explorer region's current tectonics. We use broadband data from the recently established network of three-component seismograph stations in British Columbia and the Pacific Northwest of the United States (Figure 2) to obtain the first reliable earthquake source parameter estimates for the region's frequent, moderately sized earthquakes. Combined with the Harvard centroid moment tensor solutions [*Dziewonski et al.*, 1994, and references therein], they represent the region's largest earthquake source parameter data set determined by robust waveform matching techniques. In addition, because of documented bias in routine locations [*Hyndman and Rogers*, 1981], we relocate larger earthquakes using the joint epicenter determination technique [*Douglas*, 1967; *Dewey*, 1972].

2. Methods and Results

2.1. Moment Tensors

[6] The new three-component, high-dynamic range, broadband seismic network in British Columbia and the Pacific Northwest (Figure 2) now allows seismological studies once impossible to perform with the classical short-period vertical seismometer network. In this study, we employ robust waveform fitting techniques to determine source parameters of small-medium magnitude ($M \geq 4$) earthquakes in the offshore Explorer region. Source parameter estimates based on *P* wave first-motion polarities from earlier short-period networks in western Canada and Washington are unreliable because the stations cover only a small azimuthal segment of the focal sphere.

[7] The broadband network in the Pacific Northwest, which initiated in the late 1980s with the installation of the Corvallis, Oregon station (COR), currently consists of about 15 stations and is still growing (Figure 2). Routine earthquake source parameter analysis in the Explorer region became possible only after stations in western British Columbia opened during 1993 (PGC, BBB, PMB). Since the onset of our study in 1994, the network has evolved further, most significantly with the installation of sites on Vancouver Island (PHC, OZB, CBB) and on Moresby Island (MOBC) in 1996. These new stations, close to the Explorer region, lowered the magnitude threshold for analysis from about 4.5 to 4.0 and improved the source parameter resolution.

[8] We invert for the earthquake source parameters (deviatoric seismic moment tensor and source time-function) by minimizing the least squares misfit between observed and synthetic seismograms. Strike, dip, rake, and seismic moment of the source follow directly from the moment tensor formulation [e.g., *Aki and Richards*, 1980]. The centroid depth is found by observing the misfits for a set of trial depths, usually 4 and 6 km, and continuing deeper at 3-km increments. The inversion of the complete, three-component seismograms is performed at low frequencies using data from all available stations simultaneously. At low frequencies, the regional (event-station distance $\Delta \leq 1000$ km) seismograms are dominated by guided waves and surface waves that can be adequately modeled using a relatively simple 1-D velocity depth model (Figure 2 inset). Synthetic seismograms are calculated with *Bouchon's* [1982] wave number summation technique. For more details of the method, refer to *Nábělek and Xia* [1995] and *Braunmiller et al.* [1995].

[9] The actual frequency band used for inversion depends on earthquake size and station-event distances. We adjust the band such that the signal-to-noise ratio is good, and the prominent phases of synthetic and observed seismograms are in phase. In most instances, the passband is 0.02–0.05 Hz. For larger events, when we include more distant stations, the passband is shifted to lower frequencies, while for smaller events, when long-period noise buries the signal, the passband is shifted to higher frequencies. On average, 20–25 waveforms from about 10 stations are used. We use three-component data whenever possible; however, visibly noisy traces are discarded.

[10] Since 1994, we have determined source parameters of 84 earthquakes in the Explorer region (Table 1). Several examples of waveform fits and source parameter uncertainty estimates are shown in Appendix A. The average uncertainties in strike, dip, and rake of ±5°, ±15°, and ±20°, and centroid depth of ±3 km, were estimated by observing the variance increase relative to each event's best fit model.

[11] In addition to our regional moment tensor (RMT) solutions, we used source parameter estimates from the 34 Harvard centroid moment tensor (CMT) solutions for the Explorer region from 1976 until 1998 (Table 2). For recent, larger earthquakes, both RMT and CMT solutions are available, and they generally agree very well (Appendices A and D[1]).

[1]Supporting material in Appendices D and E are available via Web browser or via Anonymous FTP from ftp://agu.org, directory ''apend'' (Username = ''anonymous'', Password = ''guest''); subdirectories in the ftp site are arranged by paper number. Information on searching and submitting electronic supplements is found at http://www.agu.org/pubs/esupp_about.html.

Table 1. Regional Moment Tensor Solutions for the Explorer Region[a]

Date	Latitude, °N	Longitude, °W	S/D/R, deg	M_0, N m	M_w	CD, km	DC, %	CO	SV, deg	SR
9401030126	49.583	127.042	254/40/332	2.83 E17	5.6	20	68	28	95	9
9402120704	49.102	129.350	131/82/157	4.02 E17	5.7	6	26	20	315	8
9404122114	50.302	130.190	324/84/211	9.43 E15	4.6	10	47	17	320	5
9404270030	48.677	129.145[b]	134/63/168	1.54 E16	4.8	8	9	18	320	8
9407150502	50.472	130.065	136/86/165	1.50 E16	4.8	10	72	14	317	4
9408211305	50.398	130.430[b]	140/86/166	4.80 E16	5.1	12	53	18	321	4
9411021352	50.515	130.286[b]	141/84/166	2.89 E15	4.3	12	91	14	323	4
9411200122	49.180	125.535[b]	301/65/130	1.92 E15	4.2	60	96	12		12
9501090650	51.045	130.737	335/63/187	1.20 E16	4.7	4	87	14	332	3
9501160701	49.971	130.096[b]	142/85/157	3.85 E15	4.4	15	43	8	324	5
9501170813	50.026	130.120[b]	148/62/168	6.76 E15	4.5	6	43	13	334	5
9501171442	50.004	130.188[b]	151/58/174	4.94 E16	5.1	6	85	15	334	5
9503081630	50.503	129.965	139/84/167	1.53 E16	4.8	12	76	14	320	4
9504230929	50.457	130.219[b]	132/87/169	4.50 E15	4.4	12	92	8	313	4
9505310338	50.931	130.683	146/79/168	5.89 E16	5.2	12	41	17	328	3
9506212024	50.919	130.747	158/61/193	1.45 E17	5.4	6	69	15	332	3
9509122244	51.143	131.200	333/86/216	7.92 E16	5.2	9	53	14	330	3
9509130759	51.312	130.900	148/90/155	1.08 E17	5.3	9	71	13	328	3
9509131119	51.092	131.034[b]	148/87/151	1.50 E16	4.8	9	62	13	330	3
9510150129	48.850	128.601[b]	310/79/214	4.82 E15	4.4	9	19	13	303	8
9510311940	50.617	130.456[b]	146/83/165	5.04 E15	4.4	12	72	13	328	4
9511121305	48.838	129.179[b]	130/67/166	1.53 E16	4.8	9	13	17	316	8
9512010329	50.363	130.038[b]	135/77/156	4.14 E15	4.4	9	78	18	321	4
9601031312	49.473	130.242	134/84/169	7.88 E16	5.2	6	72	17	315	7
9601281130	48.945	129.276[b]	135/80/161	7.72 E15	4.6	6	21	18	318	8
9603102112	50.573	130.436[b]	143/85/169	1.21 E16	4.7	12	78	26	324	4
9603162318	50.690	129.880	324/86/194	6.86 E16	5.2	12	91	28	323	4
9603180801	49.791	127.103	246/61/343	4.12 E16	5.0	15	78	37	74	9
9604231516	48.983	128.233[b]	215/62/0	3.88 E15	4.4	9	48	22	35	9
9608160341	51.097	130.645	155/88/170	4.90 E16	5.1	4	82	33	335	3
9608160954	51.150	130.670[b]	158/83/176	1.37 E16	4.7	4	85	28	338	3
9608202241	50.512	130.277[b]	323/73/192	1.06 E15	4.0	9	86	16	319	4
9608230913	47.727	129.261[c]	10/62/270	1.66 E16	4.8	9	68	39	100	11
9609092228	49.011	128.833[b]	115/75/188	1.89 E15	4.2	6	24	16	293	8
9610062013	48.965	128.208	41/86/335	2.40 E18	6.2	4	81	30	43	9
9610062029	48.863	128.144[b]	42/88/337	1.95 E16	4.8	4	56	19	43	9
9610062043	48.792	128.250[b]	227/80/12	1.75 E16	4.8	4	62	29	45	9
9610070204	48.815	128.157[b]	246/80/25	6.55 E15	4.5	4	40	38	61	9
9610070737	48.831	128.324[b]	23/88/341	5.90 E15	4.5	4	53	25	24	9
9610071018	48.944	128.259[b]	57/90/347	4.39 E15	4.4	4	86	29	57	9
9610071836	48.920	128.113[b]	189/68/349	2.07 E16	4.8	6	96	33	19	9
9610090712	49.581	129.977	147/75/153	5.77 E17	5.8	6	46	32	335	7
9610090952	49.546	129.920[b]	128/73/168	3.38 E15	4.3	9	82	20	312	7
9610131133	48.899	128.164[b]	29/86/342	2.67 E15	4.3	6	9	28	30	9
9610142304	48.841	128.203[b]	31/83/332	5.82 E15	4.5	4	29	24	35	9
9611060655	50.454	130.213[b]	323/69/199	4.42 E15	4.4	9	87	14	316	4
9611210124	49.579	128.786[b]	316/88/203	5.19 E15	4.4	6	61	27	315	10
9611210130	49.583	128.813[b]	304/79/204	1.79 E15	4.1	6	39	20	299	10
9612241240	51.867	131.715[b]	157/79/159	5.78 E15	4.5	15	43	13	341	2
9702051927	51.615	131.432	159/87/184	3.41 E16	5.0	6	63	20	339	2
9702051929	51.543	131.474	159/87/182	8.69 E16	5.3	6	87	20	339	2
9703290545	50.475	130.226[b]	324/77/189	3.85 E15	4.4	9	84	17	322	4
9703300650	50.485	130.221[b]	322/84/207	3.61 E15	4.3	6	72	19	319	4
9704132025	51.388	131.224	330/82/197	1.45 E16	4.7	9	96	25	328	3
9707100649	49.231	127.881[b]	20/75/334	3.47 E15	4.3	6	47	22	27	9
9708160623	48.848	129.196[b]	114/65/177	7.69 E15	4.6	12	79	19	295	8
9709200439	50.892	130.298	56/76/282	8.79 E16	5.3	4	69	37	325	3
9709200709	50.754	130.523	61/79/284	1.37 E17	5.4	4	61	37	331	3
9710041515	48.057	129.022[c]	120/87/232	5.53 E15	4.5	4	60	27	115	11
9710210810	50.412	130.169[b]	320/82/203	8.40 E15	4.6	9	95	26	317	4
9712200422	50.447	130.342[b]	141/89/164	9.48 E15	4.6	9	95	15	321	4
9802081911	50.499	130.287[b]	323/79/197	4.80 E15	4.4	9	81	23	320	4
9802140545	50.845	130.505[b]	156/66/199	4.49 E15	4.4	4	52	22	328	3
9802140619	50.855	130.511[b]	154/51/179	5.03 E15	4.4	4	60	18	335	3
9802181846	49.543	129.858[b]	131/80/160	1.02 E16	4.6	12	57	21	315	7
9806122024	48.892	129.032[b]	122/83/170	5.67 E15	4.5	9	68	17	304	8
9806252251	50.085	130.269	144/81/160	1.21 E17	5.4	9	35	27	328	5
9806271020	49.630	127.160[b]	250/66/337	9.76 E14	4.0	24	88	23	80	9
9807100305	50.548	130.328[b]	146/83/199	1.14 E15	4.0	9	82	20	324	4
9807140105	48.728	129.144[b]	127/74/175	1.05 E16	4.7	6	54	24	308	8
9807140149	48.773	129.009[b]	128/59/179	1.04 E15	4.0	6	41	18	309	8
9807140227	48.773	129.015[b]	127/75/169	4.84 E15	4.4	6	36	22	310	8

Table 1. (continued)

Date	Latitude, °N	Longitude, °W	S/D/R, deg	M_0, N m	M_w	CD, km	DC, %	CO	SV, deg	SR
9807150030	47.821	129.285[c]	5/57/261	1.17 E16	4.7	6	72	33	103	11
9807310740	51.362	130.782[b]	158/71/177	7.72 E15	4.6	6	96	23	339	3
9807310818	51.341	130.798[b]	153/79/178	1.30 E15	4.0	6	63	22	333	3
9808060243	52.126	131.664[b]	312/37/110	5.04 E15	4.4	15	32	20	18	1
9808061811	48.789	129.223[b]	116/70/172	8.03 E15	4.6	12	72	20	299	8
9808061817	48.885	129.349[b]	119/68/173	1.89 E16	4.8	9	39	23	302	8
9808161925	50.009	130.245[b]	144/61/170	2.14 E15	4.2	9	71	21	329	5
9808190439	50.386	130.338[b]	321/79/191	2.37 E16	4.9	9	93	27	319	4
9808301133	50.969	130.658	160/50/181	1.92 E18	6.2	4	61	34	339	3
9809010743	50.901	130.710[b]	327/84/180	2.34 E15	4.2	9	80	19	327	3
9809010919	49.143	127.775[b]	49/78/323	3.92 E15	4.4	6	32	31	58	9
9809011812	50.732	130.584[b]	156/63/189	1.01 E16	4.6	6	43	24	332	4

[a]Date is year month day hour minute. Latitude and longitude are relocated latitude and longitude (unless otherwise indicated). S/D/R are strike, dip, and rake. M_0 is seismic moment; read 2.83 E17 as 2.83×10^{17}. M_w is moment magnitude. CD is centroid depth. DC is double-couple percentage. DC = $(1-2\varepsilon) \times 100$ [%], ε = |smallest|/|largest| moment tensor eigenvalue. CO is number of components (vertical, radial, and transverse) used. SV is slip vector azimuth. SR is source region. 1, Queen Charlotte Islands; 2, NW of TW seamounts; 3, TW seamounts to Dellwood knolls; 4, Dellwood knolls to Explorer rift; 5, Explorer rift; 6, Explorer deep; 7, north of western Sovanco; 8, eastern Sovanco; 9, Nootka transform; 10, inside Explorer plate; 11, Juan de Fuca ridge; 12, Juan de Fuca-North America subduction zone.

[b]Located by Pacific Geoscience Centre, Sidney, British Columbia, Canada.

[c]Located by NOAA PMEL, Newport, Oregon.

Table 2. Harvard Centroid Moment Tensor Solutions for the Explorer Region[a]

Date	Latitude, °N	Longitude, °W	S/D/R, deg	M_0, N m	M_w	CD, km	DC, %	SV, deg	SR
7602231514	51.452	130.656	355/80/191	1.14 E18	6.0	23	82	353	1
7612202033	48.766	129.405	127/89/181	1.20 E19	6.7	15[b]	90	307	8
7806111455	49.156	129.691	315/90/180[c]	3.37 E18	6.3	11	76	315	8
7807110255	52.647	132.236	296/28/79	1.34 E17	5.4	15[b]	98	26	1
7903130951	49.770	130.177	330/90/180[c]	1.63 E17	5.4	10	92	330	5
7903131200	49.802	130.027	315/90/180[c]	3.94 E17	5.7	10	98	315	5
7906211703	51.107	130.973	323/88/171	2.23 E17	5.5	15[b]	72	323	3
8005162234	49.593	128.191	300/90/180[c]	1.24 E17	5.4	15[b]	86	300	10
8010020342	50.115	130.394	345/90/180[c]	2.23 E17	5.5	15[b]	46	345	5
8012171621	49.417	129.888	326/90/180[c]	1.40 E19	6.7	10	80	326	7
8205151848	50.178	130.438	331/90/180[c]	5.80 E17	5.8	10	96	331	5
8406242133	50.916	130.914	160/80/188	6.12 E17	5.8	10	88	339	3
8408120024	50.086	130.258	142/76/181	1.10 E17	5.3	10	50	321	5
8805261901	48.886	128.765	116/88/178	7.59 E16	5.2	15[b]	52	296	8
8807191054	50.391	130.234	167/87/175	2.98 E17	5.6	15[b]	66	347	4
8811270036	50.614	130.470	319/41/178	3.24 E17	5.6	15[b]	26	321	4
9002030954	50.834	130.542	338/90/180[c]	2.01 E17	5.5	15[b]	52	338	3
9002161328	49.033	127.972	208/85/12	1.41 E17	5.4	15[b]	98	27	9
9107170712	50.692	130.636	329/80/176	2.19 E17	5.5	15[b]	72	330	4
9201021640	48.602	129.610	315/90/174	1.30 E18	6.0	23	76	315	8
9201130608	49.060	129.212	306/75/203	1.28 E17	5.4	15[b]	64	300	8
9204061354	50.55	130.46	331/73/191	1.19 E19	6.7	15[b]	90	328	4
9204061516	50.490	130.318	166/76/181	1.02 E18	6.0	15[b]	72	346	4
9204070042	50.663	131.116	354/90/180[c]	8.24 E16	5.2	15[b]	82	354	13
9204230540	51.341	131.108	327/52/180	3.14 E17	5.6	15[b]	50	327	3
9308030719	51.157	130.745	355/60/194	1.22 E18	6.0	15[b]	100	347	3
9401030126[d]	49.583	127.042	251/41/334	2.89 E17	5.6	21	92	91	9
9506212024[d]	50.919	130.747	161/90/175	1.51 E17	5.4	15[b]	64	341	3
9610062013[d]	48.965	128.208	46/86/8	2.21 E18	6.2	15[b]	72	45	9
9610090712[d]	49.581	129.977	332/72/184	5.22 E17	5.8	15[b]	100	331	7
9702051929[d]	51.543	131.474	350/75/200	7.36 E16	5.2	15[b]	85	345	2
9709200709[d]	50.754	130.523	347/63/189	7.63 E16	5.2	15[b]	31	342	3
9806252251[d]	50.085	130.269	328/90/180[c]	9.60 E16	5.3	15[b]	68	328	5
9808301133[d]	50.969	130.658	346/82/180	1.45 E18	6.1	15[b]	83	346	3

[a]Date is year month day hour minute. Latitude and longitude are relocated latitude and longitude. Source information is taken from *Dziewonski et al.* [1994] and related sources. S/D/R are strike, dip, and rake; M_0 is seismic moment; read 1.14 E18 as 1.14×10^{18}. M_w is moment magnitude. CD is centroid depth; DC is double-couple percentage. SV is slip-vector azimuth. SR is source region. 1, Queen Charlotte Islands; 2, NW of TW seamounts; 3, TW seamounts to Dellwood knolls; 4, Dellwood knolls to Explorer rift; 5, Explorer rift; 6, Explorer deep; 7, north of western Sovanco; 8, eastern Sovanco; 9, Nootka transform; 10, inside Explorer plate; 11, Juan de Fuca ridge; 12, Juan de Fuca-North America subduction zone; 13, Pacific intraplate.

[b]Constrained centroid depth.

[c]Constrained $M_{xz} = M_{yz} = 0$.

[d]RMT exists (see Table 1).

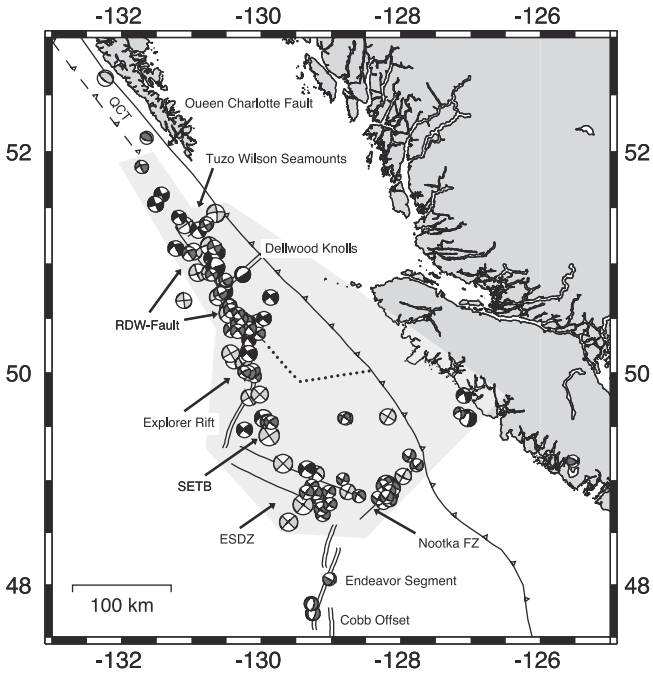

Figure 3. Map of fault plane solutions (lower-hemisphere projections, size proportional to M_w). Black symbols represent relocated regional moment tensor (RMT) solutions with relocation epicenter uncertainties $\leq$12 km. Dark gray are RMT solutions with larger relocation uncertainties and therefore placed on their Pacific Geoscience Centre locations. The three Juan de Fuca ridge events were located by NOAA. Light gray are relocated Harvard centroid moment tensor (CMT) solutions. All events are listed in Tables 1 and 2. Abbreviations are QCT for Queen Charlotte Terrace, RDW for Revere-Dellwood-Wilson, SETB for Southwest Explorer Transform Boundary, ESDZ for Eastern Sovanco Deformation Zone, FZ for fault zone.

[12] The majority of the RMT and CMT solutions inside the Explorer region (shaded region in Figure 3) have a strike-slip source mechanism. This implies that most earthquakes strong enough for moment tensor analysis ($M \geq 4$) occurred along transform faults or within the plates. Spreading segments are either aseismic, or earthquakes are too small for analysis.

[13] Before our RMT analyses, hypocenter depths for only a few earthquakes in the Explorer region were well determined. For the small earthquakes, centroid and hypocenter depths are roughly equivalent; and the centroid depth distribution (Figure 4) indicates that the seismogenic fault width in the Explorer region is about 10 km. This agrees well with hypocenter depth estimates from ocean bottom seismometer studies [*Hyndman and Rogers*, 1981] and a shallow 4–5 km centroid depth estimate for the M_w = 6.7, 920406 earthquake on the Revere-Dellwood-Wilson fault [*Cassidy and Rogers*, 1995].

2.2. Earthquake Slip Vectors

[14] Earthquake slip vector azimuths describe relative plate motion directions and are a key to understanding the region's current tectonics. We derived the slip vectors from the fault plane solutions by choosing the nodal plane as the fault plane that agrees best with local geology. For the strike-slip earthquakes in the Explorer region, slip vector azimuth uncertainties depend mainly on uncertainties in strike, which is the best resolved source parameter (±5°). The slip vector azimuths, with uncertainties of only about 5°, define the current plate motion directions tightly.

[15] Figure 5 shows slip vector azimuths from Explorer region's boundary with the Pacific plate (gray shaded area), their average (line AVE), and predicted plate motion directions based on two existing models (lines PAC-NAM and PAC-EXP/R). If the Explorer region were cut by a Pacific-North America transform fault [*Barr and Chase*, 1974; *Rohr and Furlong*, 1995], the slip vector azimuths would follow Pacific-North American relative motion (340° azimuth, line PAC-NAM). If the Explorer region were moving in *Riddihough's* [1984] Explorer plate sense, the slip vector azimuths would follow Pacific-Explorer relative motion (310° azimuth, line PAC-EXP/R). However, most observations and their average (line AVE) point in a 325° direction, which is incompatible with either model.

[16] Splitting the Explorer-Pacific boundary in five segments shows that the slip vector azimuths (thin solid lines,

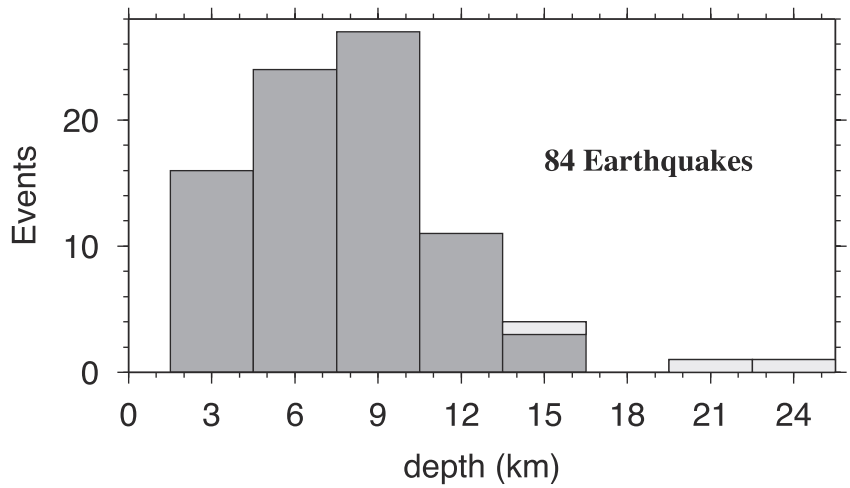

Figure 4. Earthquake centroid depths of the RMT solutions. The lightly shaded bars represent three events near Nootka Island where Juan de Fuca and presumably Explorer plate subduct beneath North America.

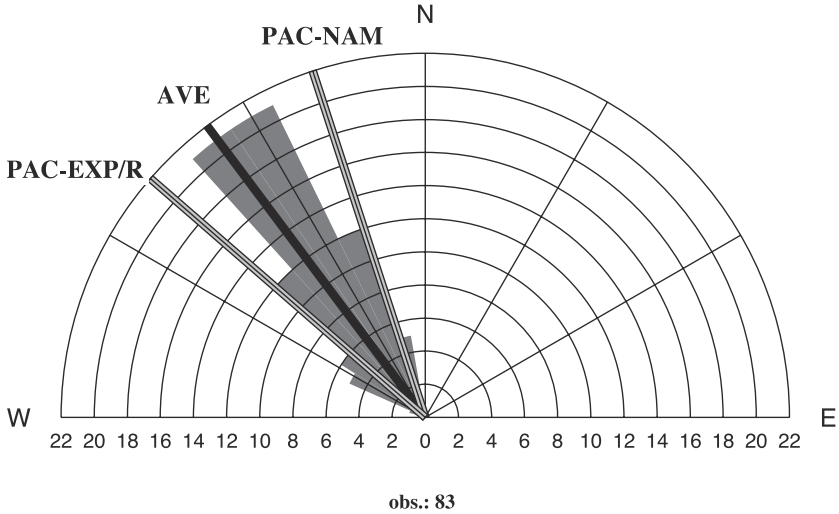

Figure 5. Earthquake slip vector azimuths along the Explorer-Pacific boundary (regions 2–8 in Tables 1 and 2). The observed azimuths (gray shaded) are binned in 8° intervals. Semicircles show the number of events per bin. The observed azimuths and their average of 323° (labeled AVE) are incompatible with Pacific-North America motion (340°, labeled PAC-NAM) and *Riddihough*'s [1984] Pacific-Explorer motion (310°, labeled PAC-EXP/R).

Figure 6) rotate counterclockwise from a north-northwest direction in the north to a northwest direction in the south. For each segment, the average slip vector azimuth (solid line) corresponds well with the observed fault trend (dashed line), but is incompatible with Pacific-North America motion (gray PAC-NAM line) or *Riddihough*'s [1984] predicted Explorer-Pacific plate motion (gray PAC-EXP/R line). Figure 6 will be discussed in more detail later in the text.

[17] Our results differ substantially from those published recently by *Kreemer et al.* [1998]. This difference is discussed in electronic supporting material Appendix E.

2.3. Epicenter Relocations

[18] Routine earthquake locations in the Explorer region (Figure 2) are widely scattered and often far from morphologic features usually associated with offshore plate boundaries. This observation was used to argue that the bathymetric features are inactive remnants, no longer representing active plate boundaries, and that the earthquakes define a new Pacific-North America transform plate boundary [*Barr and Chase*, 1974; *Rohr and Furlong*, 1995]. However, ocean bottom seismometer studies and small-earthquake ($3 \leq M \leq 5$) relocations reveal narrowly distributed earthquakes closely following morphologically identified tectonic features, indicating that routine land-based epicenter locations are systematically mislocated by tens of kilometers to the northeast [*Hyndman and Rogers*, 1981; *Wahlström and Rogers*, 1992].

[19] The locations of larger, tectonically more significant earthquakes, a key to deciphering current plate boundaries, had not been well determined. We thus relocated larger earthquakes in the Explorer region with the joint epicenter determination (JED) technique [*Douglas*, 1967; *Dewey*, 1972].

[20] We simultaneously relocated 164 earthquakes using *P* wave arrival time data from the International Seismological Centre (ISC), available from 1964 until 1987, and from the US Geological Survey (monthly and weekly PDE) since then. Only events with at least 30 teleseismic (event-station distance $18° \leq \Delta \leq 110°$) arrival time picks and events with a CMT or RMT solution (even if less than 30 picks were available) were included. The 30 P wave pick criterion is essentially equivalent to relocating all $M > 5.0$ earthquakes. Because of the poor hypocenter depth resolution offered by teleseismic data, we fixed all depths to 10 km except the deeper 940103 event near Nootka Island, whose depth is well constrained by the Pacific Geoscience Centre (PGC) location (24 km) and our RMT solution (20 km).

[21] To stabilize the JED inversion, we picked an independently well-located earthquake, fixed its location, and relocated all other earthquakes relative to it. We chose the M_w = 6.7, 920406 earthquake on the Revere-Dellwood-Wilson fault because it was carefully located [*Cassidy and Rogers*, 1995] and has the most P arrival time picks of all events in our study. We tried other well-located earthquakes as reference events (such as the 940103 earthquake near Nootka Island located by the PGC with local network data) and obtained very similar relocations.

[22] The relocated epicenters (Figure 7), shown as open circles with thin lines pointing to the original epicenters, are on average about 25 km southwest of their original locations. This average difference is consistent with the reference event's epicenter (star, Figure 7) [*Cassidy and Rogers*, 1995] about 30 km southwest of its Preliminary Determination of Epicenters (PDE) location. Relocation moved the epicenters from inside the Explorer region toward tectonic features; more detailed inspection shows relocation also adjusted relative event locations, reducing the epicenter scatter.

[23] The 113 well-relocated epicenters, for which latitude and longitude uncertainties are less than 12 km at the 95% confidence level, reveal Explorer region's plate boundaries (Figure 8). We are confident in the overall location quality because seismicity and bathymetry correspond well. Partic-

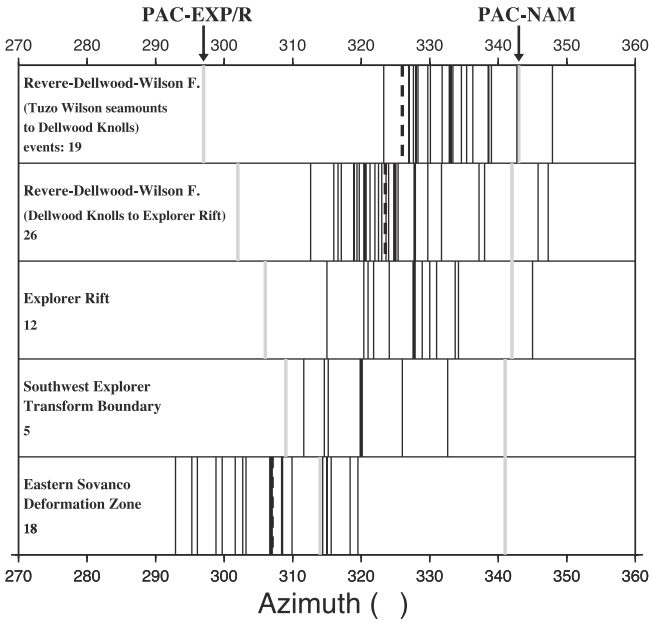

Figure 6. Slip vector azimuth distribution along five Explorer-Pacific boundary segments. First panel, Revere-Dellwood-Wilson (RDW) fault from Tuzo Wilson (TW) seamounts to Dellwood Knolls (DK) (region 3 in Tables 1 and 2). Second panel, RDW fault between DK and Explorer Rift (ER) (region 4). Third panel, transform faults in ER section (region 5). Fourth panel, Southwest Explorer Transform Boundary north of western Sovanco fracture zone (region 7). Fifth panel, Eastern Sovanco Deformation zone (region 8). For each panel, thin solid lines are observed earthquake slip vector azimuths, the thick solid line is their average, and the dashed line shows the active fault trend determined from the bathymetry. The gray lines represent predicted Pacific-North America (PAC-NAM, NUVEL-1 [*DeMets et al.*, 1990]) and *Riddihough*'s [1984] Pacific-Explorer (PAC-EXP/R) motion directions. There is good correspondence between average slip vector azimuth and bathymetry for each panel. The observed azimuths differ substantially from both PAC-NAM and PAC-EXP/R predicted motion.

ularly striking are the locations along Explorer Rift, which follow the bathymetrically defined rift very closely. Also, PGC's earthquake locations close to Nootka Island (well constrained by local seismic stations on Vancouver Island) generally fall inside the confidence limits. Another indicator for good location quality comes from earthquakes near Brooks peninsula. There, the relocations agree with locally recorded aftershock epicenters [*Spindler et al.*, 1997]. The remaining epicenter scatter in Figure 8 (along the northwest part of the Revere-Dellwood-Wilson fault and in the eastern Sovanco fracture zone) and the deviation from bathymetric features (north of the western Sovanco fracture zone) appear to be real.

[24] The relocations form a band roughly parallel to the Pacific-North America plate motion direction seemingly supporting the Pacific-North America transform hypothesis [*Barr and Chase*, 1974; *Rohr and Furlong*, 1995]. However, the slip vector azimuths (Figure 6) are less northerly than the

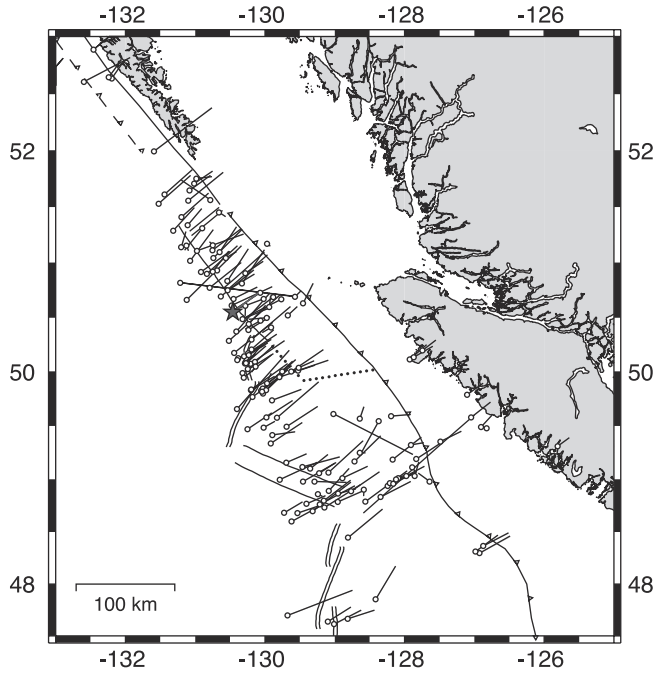

Figure 7. Epicenter relocations. Open circles are relocated epicenters with the thin lines pointing to the original epicenters. Star shows the location of the reference event [*Cassidy and Rogers*, 1995] with the thick gray line pointing to its PDE location.

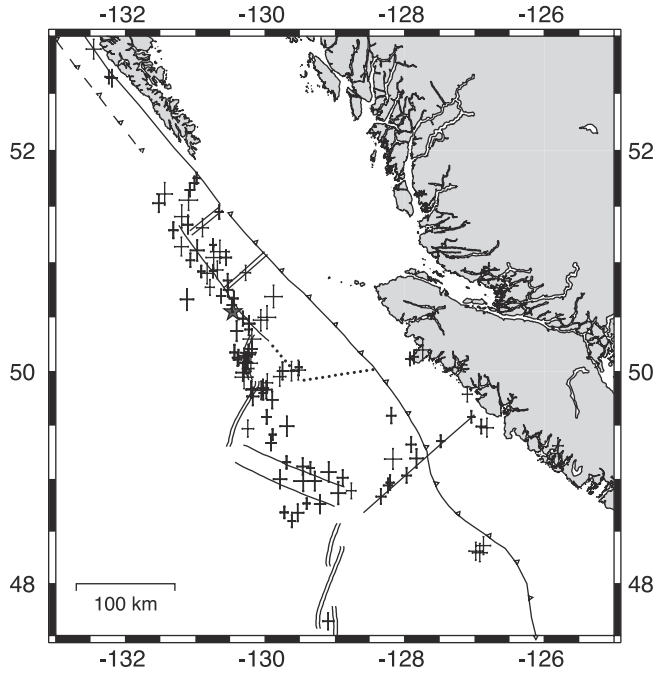

Figure 8. Uncertainty bars of 113 well-relocated earthquakes (events with latitude and longitude uncertainties $\leq$12 km at 95% confidence level). Thick bars mark $M \geq 5$ earthquakes. Star shows the reference event location [*Cassidy and Rogers*, 1995].

Pacific-North America motion direction. This suggests that several right-stepping strike-slip faults, each parallel to the slip vector azimuths, are active with the overall seismicity apparently following a more northerly trend.

3. Discussion of Individual Plate Boundary Segments

3.1. Queen Charlotte Transform Fault

[25] The right-lateral Queen Charlotte transform fault forms the Pacific-North America plate boundary north of the Explorer region. North of the Queen Charlotte Islands, the fault is parallel to the plate motion direction (NUVEL-1 [*DeMets et al.*, 1990]), and motion is purely strike-slip (Figures 1 and 3). Going south, a counter-clockwise fault bend at the Queen Charlotte Islands (Figures 1 and 3) results in a 20° difference between fault trend and plate motion direction, requiring oblique Pacific-North America plate convergence along the southern Queen Charlotte fault.

[26] Slip partitioning into strike-slip motion along, and convergent motion perpendicular to, the southern Queen Charlotte fault has been suggested to account for the oblique plate motions [*Hyndman et al.*, 1982; *Scheidhauer*, 1997]. The Queen Charlotte fault, which runs close to the coast off Queen Charlotte Islands (Figure 8, also *Hyndman and Ellis* [1981], *Bérubé et al.* [1989], *Scheidhauer* [1997]), is separated by a 20–30 km wide terrace from the Pacific plate. Presumably this terrace is decoupled from either of the main plates: the Pacific plate subducts at the terrace's oceanward side and the terrace translates northwest relative to North America along the Queen Charlotte fault [*Hyndman et al.*, 1982; *Scheidhauer*, 1997]. The three earthquake source mechanisms along the fault's southern part, two thrust and one strike-slip (Figure 3), are consistent with slip partitioning. Additional support for Pacific plate underthrusting comes from numerous morphological, seismic, and potential field data and flexural modeling [*Chase et al.*, 1975; *Hyndman and Ellis*, 1981; *Hyndman et al.*, 1982; *Riddihough*, 1982; *Yorath and Hyndman*, 1983; *Horn et al.*, 1984; *Dehler and Clowes*, 1988; *Bérubé et al.*, 1989; *Mackie et al.*, 1989; *Sweeney and Seemann*, 1991]. Relatively high seismicity on and east of Graham Island [*Bérubé et al.*, 1989; *Bird and Rogers*, 1996] and compression in the Queen Charlotte basin [*Rohr and Dietrich*, 1992] indicate that some Pacific-North America deformation also occurs within the North American plate considerably east of the Queen Charlotte fault. *Rohr et al.* [2000] argue against Pacific plate's underthrusting, and instead, propose down warping and crustal thickening on both sides of the fault. The locations and low dips of the two thrust earthquakes we studied support the underthrusting model, but do not exclude *Rohr et al.*'s [2000] model.

[27] *Hyndman and Rogers* [1981] and *Carbotte et al.* [1989] discuss the possibility of the Queen Charlotte fault extending as far south as the Dellwood Knolls. Earthquake epicenters (Figure 9) indicate that the active Queen Charlotte fault terminates near the Tuzo Wilson seamounts.

3.2. Revere-Dellwood-Wilson Transform Fault

[28] The seismically very active Revere-Dellwood-Wilson transform fault (Figure 9) forms the right-lateral boundary between the Pacific plate and Explorer region. The fault, visible on side-scan images from the Tuzo Wilson seamounts to Explorer Deep [*Carbotte et al.*, 1989; *Davis and Currie*, 1993], is almost parallel to the southern Queen Charlotte fault and thus cannot accommodate the entire, more northerly oriented, Pacific-North America motion. The remaining convergent motion requires either slip-partitioning comparable to the setting along southern Queen Charlotte fault, the fault is then a Queen Charlotte fault extension and forms the Pacific-North America boundary; or the Pacific and North American plates are separated by the Explorer plate, the fault is then a Pacific-Explorer transform boundary and convergence occurs between the Explorer and North American plates. Compressional bathymetric features, similar to the terrace oceanward of the southern Queen Charlotte fault, do not exist southwest of the Revere-Dellwood-Wilson fault [*Carbotte et al.*, 1989], thus favoring Explorer-North America convergence northeast of the fault.

[29] Seismicity along the Revere-Dellwood-Wilson fault extends from northwest of the Tuzo Wilson seamounts to its intersection with the Explorer Rift (Figure 9). Between the Dellwood Knolls and the Explorer Rift the epicenters are tightly focused on the Revere-Dellwood-Wilson fault, which is consistent with earlier results [*Hyndman and Rogers*, 1981; *Wahlström and Rogers*, 1992; *Cassidy and Rogers*, 1995]. The source mechanisms, except for two normal faulting events, are strike-slip, and their slip vector azimuths (average 325°, Figure 6) agree very well with the 323° fault trend [*Davis and Currie*, 1993]. This close agreement between the earthquake epicenters, slip vectors and the geology discerned from high-resolution SeaBeam bathymetry was also a reason for selecting the master event for our relocations from this group of events. The seismicity stops abruptly at the Revere-Dellwood faults' intersection with the Explorer Rift (Figure 9) [*Hyndman and Rogers*, 1981; *Wahlström and Rogers*, 1992; *Cassidy and Rogers*, 1995], suggesting the fault continuation, visible on side-scan data along the oceanward side of the Paul Revere Ridge to Explorer Deep [*Davis and Currie*, 1993], is inactive.

[30] North of the Dellwood Knolls, up to the Tuzo Wilson seamounts, the earthquake epicenters are much more scattered. The slip vector azimuths of the strike-slip events are on average (332°, Figure 6) slightly more northerly than the 326°-trending Revere-Dellwood-Wilson fault trace visible on side-scan images [*Carbotte et al.*, 1989], indicating that several faults are active simultaneously. Several strike slip earthquakes clearly suggest an extension of the Revere-Dellwood-Wilson fault system beyond the Tuzo Wilson seamounts. Although initially considered inactive [*Carbotte et al.*, 1989], this extension is visible on seismic reflection images for about 50 km past the seamounts. Scattered seismicity between the Tuzo Wilson seamounts and the Dellwood Knolls could probably be the result of ongoing pull-apart tectonism in which the lengthening Revere-Dellwood-Wilson fault system tries to connect to the retreating Queen Charlotte fault by distributing transform motion along several fault strands. A small volcanic field 30 km northwest of the Tuzo Wilson seamounts [*Carbotte et al.*, 1989; *Allan et al.*, 1993] is consistent with the suggested northwest migration of the pull-apart extension.

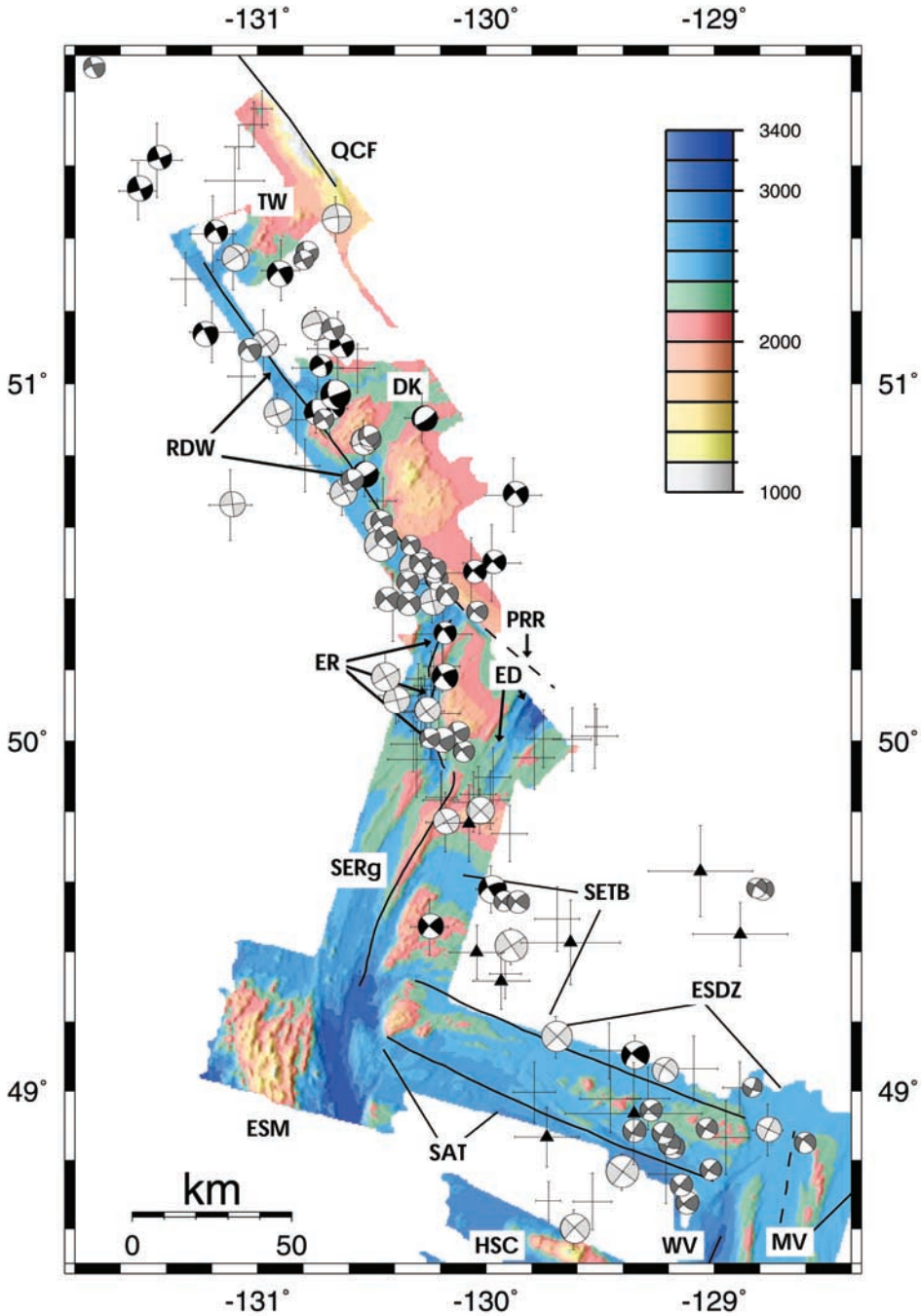

Figure 9. Close-up of the Pacific-Explorer boundary. Plotted are fault plane solutions (gray scheme as in Figure 3) and well-relocated earthquake epicenters. The SeaBeam data are from the RIDGE Multibeam Synthesis Project (http://imager.ldeo.columbia.edu) at the Lamont-Doherty Earth Observatory. Epicenters labeled by solid triangles are pre-1964, historical earthquakes (see Appendix B). Solid lines mark plate boundaries inferred from bathymetry and side-scan data [*Davis and Currie*, 1993]; dashed were inactive. QCF is Queen Charlotte fault, TW are Tuzo Wilson seamounts, RDW is Revere-Dellwood-Wilson fault, DK are Dellwood Knolls, PRR is Paul Revere ridge, ER is Explorer Rift, ED is Explorer Deep, SERg is Southern Explorer ridge, ESM is Explorer seamount, SETB is Southwest Explorer Transform Boundary, SAT is Southwestern Assimilated Territory, ESDZ is Eastern Sovanco Deformation Zone, HSC is Heck seamount chain, WV is active west valley of Juan de Fuca ridge, MV is inactive middle valley.

[31] The Tuzo Wilson seamounts and the Dellwood Knolls, both young volcanic fields, are considered to be active seafloor spreading centers [*Riddihough et al.*, 1980; *Davis and Riddihough*, 1982; *Cousens et al.*, 1985; *Carbotte et al.*, 1989] or large-scale pull-apart structures [*Allan et al.*, 1993; *Rohr and Furlong*, 1995]. *Rohr and Furlong* [1995] suggested pull-apart activity has migrated from the Dellwood Knolls [*Allan et al.*, 1993] to the Tuzo Wilson seamounts [*Cousens et al.*, 1985; *Carbotte et al.*, 1989; *Allan et al.*, 1993] during the last 2 Myr.

[32] Our teleseismic epicenter relocations indicate that seismic activity directly at the Tuzo Wilson seamounts and the Dellwood Knolls is low for moderate $M \geq 4$ earthquakes (Figure 9). Two normal faulting earthquakes near the Dellwood Knolls support some active extension. Their locations, however, are somewhat ambiguous since the regional data suggest that these two events occurred much closer to each other than their teleseismic relocations. Accepting the regional locations, these two events could be interpreted as occurring on a small extensional jog of the Revere-Dellwood-Wilson fault.

3.3. Explorer Rift and Explorer Deep

[33] Seismicity follows Explorer Rift's bathymetry closely (Figure 9). *Botros and Johnson* [1988] suggest that the Explorer Rift consists of three distinct parts: two short Explorer-Pacific spreading segments, almost perpendicular to the Revere-Dellwood-Wilson fault, and a pull-apart basin, connecting the segments with the Southern Explorer Ridge. Strike-slip source mechanisms imply the earthquakes occurred on transform faults connecting the spreading segments or bordering the pull-apart basin. The transform slip vector azimuths (average 328°, Figure 6), which agree with slip vectors from the Revere-Dellwood-Wilson fault, and the spreading segment orientations along the Explorer Rift, suggest that the Explorer Rift and Revere-Dellwood-Wilson fault are both part of the Pacific-Explorer plate boundary.

[34] Several earthquakes (Figure 9) and fresh basalts [*Cousens et al.*, 1984; *Michael et al.*, 1989] inside Explorer Deep indicate that the former seafloor spreading center, abandoned only 0.3 Myr ago [*Botros and Johnson*, 1988], is not yet entirely dormant. These earthquakes occurred prior to our moment tensor investigation, and the lack of source mechanisms prohibits clearer tectonic interpretation.

[35] The ridge jump (0.3 Myr ago) rendered the segment of the Revere-Dellwood-Wilson fault between Explorer Rift and Explorer Deep inactive. This abandoned segment, still visible on side-scan images along the southwest side of the Paul Revere ridge [*Davis and Currie*, 1993], is less northerly oriented than the remainder of the Revere-Dellwood-Wilson fault northwest of the Explorer Rift. Shifting spreading west to the Explorer Rift, thus, stopped oblique motion, which probably had caused Paul Revere ridge uplift during the last 2 Myr [*Kulm et al.*, 1973], and simplified Pacific-Explorer interactions.

3.4. Southwest Boundary of the Explorer Plate

[36] Earthquake epicenters along Explorer plate's southwest boundary are located east of the Southern Explorer Ridge and north of the western Sovanco fracture zone (Figure 9). The source mechanisms are strike-slip (Figure 9). Their slip vector azimuths (average 320°) agree with the slip vector azimuths for events along the Revere-Dellwood-Wilson fault and Explorer Rift, and with the Revere-Dellwood-Wilson fault trend (Figure 6).

[37] Southern Explorer Ridge and western Sovanco fracture zone, plate boundaries in *Riddihough*'s [1984] Explorer plate model, appear seismically inactive. To confirm that the lack of seismicity along the western Sovanco fracture zone is not an artifact of the relatively short 30-year observation period, we relocated large, older (1918–1963) earthquakes (Appendix B), which potentially could have occurred in this region. We found that all well-constrained historic earthquakes are consistent with the more recent seismicity pattern (Figure 9).

[38] Seismicity and source mechanisms thus indicate a new Pacific-Explorer transform boundary, cutting through Explorer region's southwest corner, has formed. In this process, a triangular area, bordered by the Southern Explorer Ridge (south of about 49.7°N), western Sovanco fracture zone (west of about 129.8°), and the new transform fault, has been transferred from the Explorer to the Pacific plate. We will refer to this region as the Southwestern Assimilated Territory (SAT). Seismicity along the new boundary, which we refer to as the Southwest Explorer transform boundary (SETB) (Figure 9), is dispersed, indicating that several strike-slip faults could be active. The orientation of the faults roughly parallel to the Revere-Dellwood-Wilson fault is constrained by the source mechanisms. Disrupted magnetic lineations east of Explorer ridge [*Botros and Johnson*, 1988; *Rohr and Furlong*, 1995] and a magma-starved southern end of Explorer ridge [*Michael et al.*, 1989] are consistent with recent cessation of spreading along the Southern Explorer Ridge, formation of a new transform fault (or faults) and support assimilation of the SAT by the Pacific plate.

3.5. Eastern Sovanco Fracture Zone

[39] The epicenter distribution, slip vector azimuths and bathymetry along the eastern Sovanco fracture zone are distinct from other segments along the Explorer region-Pacific plate boundary. We refer to this area as the Eastern Sovanco Deformation Zone (ESDZ). Relocated earthquakes within the ESDZ are broadly distributed (Figure 9). The seismically active area includes an anomalously wide fault zone characterized by numerous rhomb-shaped fault bounded blocks (Figure 10) [*Cowan et al.*, 1986; *Davis and Currie*, 1993] and extends south to the Heck seamount chain. Detailed bathymetry (Figure 10) shows that the northwest trending nodal planes of the earthquake fault plane solutions (average trend 306°) are roughly parallel to the northwest trending fault scarps (307°), whereas the northeast trending fault scarps (55°) and the corresponding nodal planes (average trend 37°) are not, suggesting the northwest trending scarps are the ones seismically active. The slip vector azimuths (average 308°, Figure 6) and fault trends are less northerly oriented than those along the Revere-Dellwood-Wilson, Explorer Rift or Southwest Explorer segments (Figure 6) indicating that the ESDZ does not move in quite the same sense as the rest of Explorer plate.

[40] Most earthquakes occurred in the northern part (north of about 48.8°N) of the ESDZ characterized by elevated fault bounded blocks. Several events, though,

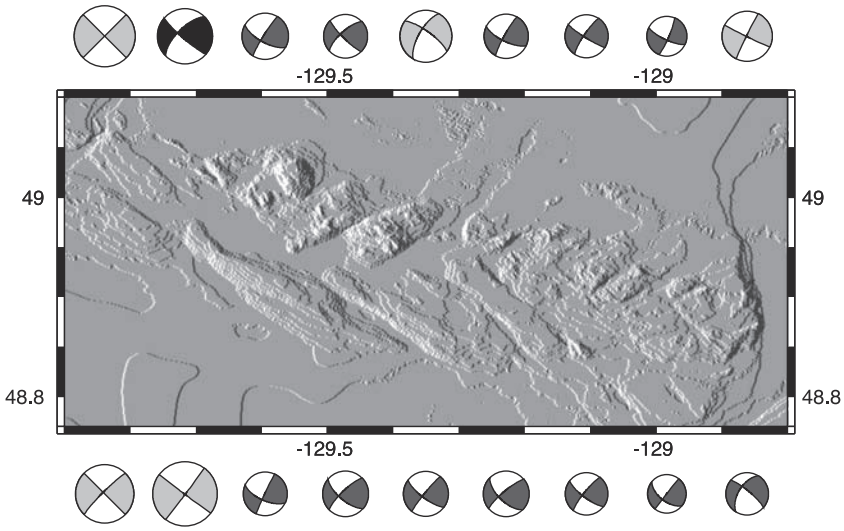

Figure 10. Detailed map of Eastern Sovanco Deformation Zone showing uplifted faulted blocks. The orientations of the northwest trending bounding faults and earthquake nodal planes agree, whereas northeast trending scarps are more easterly oriented than the northeast trending nodal planes (fault plane solution gray scheme as in Figure 3; see Figure 9 for event location). Thus it is probably the dominant northwest trending faults that move during larger earthquakes. However, some motion on the northeasterly oriented faults is required to fully account for the present Explorer-Pacific plate motion.

occurred close to the Heck seamount chain, indicating that distributed deformation extends at least south to 48.6°N. Detailed SeaBeam bathymetry is not available, but earlier work [*Barr and Chase*, 1974; *Davis and Lister*, 1977] shows the area between Heck seamount chain and the elevated blocks is filled with flat laying turbidite sediments, making geological interpretations more difficult. The striped magnetic anomaly pattern on the Pacific plate cannot be traced north of 48.5°N near the Sovanco fracture zone [*Botros and Johnson*, 1988; *Wilson*, 1993]. *Wilson* [1993] suggested this could be the result of disruption or overprinting of magnetization due to strong shearing in a former position of the Sovanco fracture zone between 48.5°N and 49°N. Earthquake activity suggests deformation is ongoing.

3.6. Nootka Fault Zone

[41] The Nootka fault zone, running from the northern tip of the Juan de Fuca ridge to Nootka Island, forms Explorer region's southeast boundary with the Juan de Fuca plate. The narrow band of relocated epicenters (Figure 11) contrasts with a broader epicenter distribution reported by *Wahlström and Rogers* [1992]. The left-lateral strike-slip source mechanisms (Figure 11) indicate transform motion, consistent with the small bathymetric relief across the fault [*Hyndman et al.*, 1979].

[42] Seismicity ends near Nootka Island. Earthquakes nearby are deeper ($\geq$15 km, Figure 4 [*Cassidy et al.*, 1988]) and have mechanisms very similar to those observed beneath Brooks peninsula, which *Spindler et al.* [1997] interpret to be a result of compression induced by the subducting Explorer plate. This appears to be a reasonable explanation for these earthquakes. For the earthquakes near Nootka Island, an interaction with the Nootka fault may contribute to their presence.

[43] *Hyndman et al.* [1979] suggested that a left lateral offset of the ridge east of Juan de Fuca ridge's Middle Valley marks the southern intersection of a broad Nootka fault zone with the Juan de Fuca ridge. A line from this left lateral offset (Figure 11), which runs northeast in the direction of the average slip vector azimuth (37°, excluding the events near Nootka Island), encompasses most relocated epicenters along the southwest part of Nootka fault and intersects the coastline north of Nootka Island. This orientation of Nootka fault is consistent with the trend of the area near the Juan de Fuca ridge having been affected by recent faulting [*Hyndman et al.*, 1979]. A possible less northerly orientation for the Nootka fault is defined by the earthquake locations (dashed line, Figure 11). Analysis of additional earthquakes along the Nootka fault, particularly some events close to the North American continental shelf, is necessary to resolve this issue.

3.7. Northern Juan de Fuca Ridge

[44] The only relocated earthquakes along the northern Juan de Fuca ridge occurred close to the non-transform [*Karsten et al.*, 1986] Cobb offset, which separates the ridge's Endeavor and Northern Symmetrical segments (Figure 8). Two normal faulting events on the southern Endeavor segment are consistent with active spreading (an additional event occurred here in 1999 [*Johnson et al.*, 2000]); a strike-slip earthquake farther north is probably associated with a step over from the Endeavor to the West Valley spreading segment (Figure 3). South of the Cobb offset, Juan de Fuca ridge is essentially aseismic down to $M = 2.3$ [*Dziak and Fox*, 1995] with the notable exception of dike injections along the CoAxial segment 1993 [*Dziak et al.*, 1995] and the Axial volcano 1998 [*Dziak and Fox*, 1999].

4. Instantaneous Pacific-Explorer Rotation Pole

[45] We use earthquake slip vectors, which define the current Explorer plate motions relative to the surrounding

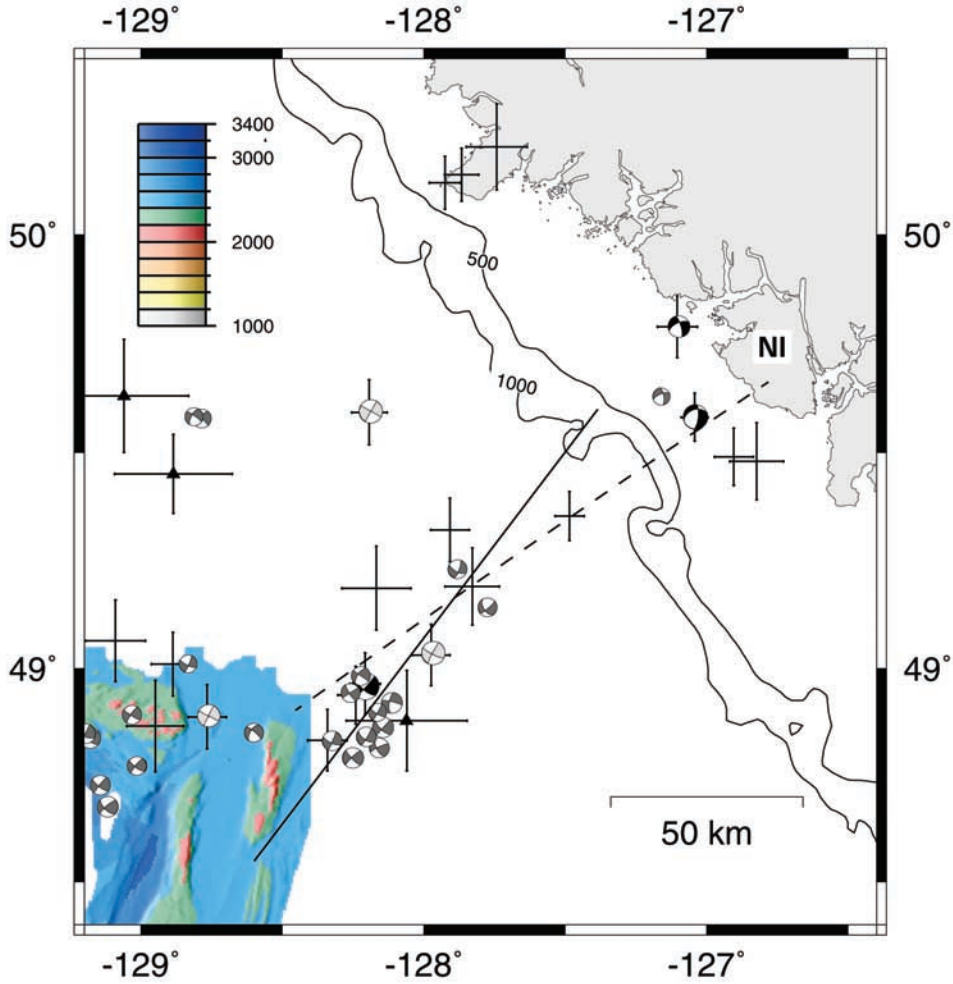

Figure 11. Close-up of the Juan de Fuca-Explorer boundary (Nootka fault). Plotted are fault plane solutions (gray scheme as in Figure 3) and well-relocated epicenters. Triangles mark pre-1964, historical earthquakes (Appendix B). High-resolution bathymetry is available only near Juan de Fuca ridge. Least squares regression of all well-relocated epicenters from Juan de Fuca Ridge to Nootka Island results in the dashed line, oriented at an azimuth of 55°. The solid line, which starts at a left-lateral offset of Juan de Fuca Ridge and trends in the direction of the average slip vector azimuth (37°, excluding earthquakes beneath Nootka Island), is consistent with the epicenter locations southwest of the continental margin. NI indicates Nootka Island.

plates, to determine the instantaneous Pacific-Explorer rotation pole. We present estimates based on two models. In model A, we use slip vector azimuths from the Explorer-Pacific boundary (excluding the ESDZ) to locate the Pacific-Explorer rotation pole. The rotation rate is estimated by using an ad hoc minimum rate constraint on the Explorer-North America motion. In model B, we include slip vector azimuths from events along Nootka fault; this added information allows location and rate of the Pacific-Explorer rotation pole to be determined.

4.1. Pacific-Explorer Rotation Pole, Model A

[46] Earthquake slip vector azimuths along the Revere-Dellwood-Wilson fault and the transform faults in the Explorer Rift and Southwest Explorer areas are similarly oriented. They agree with the morphologically defined trends along the Revere-Dellwood-Wilson fault, and change systematically from a more northerly direction along the northwestern Revere-Dellwood-Wilson fault to a more northwesterly direction along the Southwest Explorer transform(s) (top four panels Figure 6). This suggests the segments are part of the same plate boundary defining the current Explorer-Pacific plate motion direction; the systematic change implies the Pacific-Explorer rotation pole is located northeast of the Explorer region.

[47] We used a grid search, minimizing the squared misfit between observed slip vector azimuths (regions 2–5 and 7, Tables 1 and 2) and predicted plate motion directions, to locate the instantaneous Pacific-Explorer rotation pole at 54.0°N and 120.0°W (Figure 12). The location uncertainty is highly elongated perpendicular to the plate boundary (Figure 12) because slip vector azimuths along the short plate boundary change only little. Pacific-Explorer motion directions predicted by the pole agree with the slip vector azimuths and bathymetric trends (top four panels Figure 13).

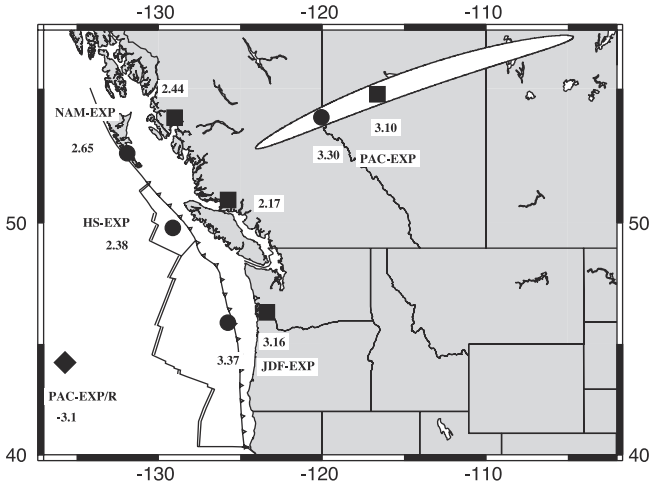

Figure 12. Explorer plate's instantaneous rotation poles. Circles are model A poles, squares are model B, and the diamond is *Riddihough*'s [1984] 0.5 Myr mean Pacific-Explorer pole. Numbers beneath poles are rotation rates in deg/Myr, positive if second plate moves counter clockwise relative to first. The ellipse surrounding model A's Pacific-Explorer pole depicts the area where the mean misfit between observed and calculated slip vector directions differs by less than 5% from the best solution (mean misfit of 8.0°); the ellipse for model B's pole is similar. Abbreviations: EXP for Explorer, PAC for Pacific, NAM for North America, JDF for Juan de Fuca, and HS for hot spot framework. See Table 3 for derivation of NAM-EXP, HS-EXP, and JDF-EXP poles.

[48] The Pacific-Explorer rotation rate can be estimated by closing the velocity triangle at the Pacific-North America-Explorer triple junction (at the Tuzo Wilson seamounts near 51.5°N, 131.0°W). At the triple junction, North America moves 4.6 cm/yr to the south-southeast (azimuth 164°; NUVEL-1A [*DeMets et al.*, 1994]) and Explorer plate moves, according to our pole location, to the southeast (azimuth 155°) relative to the Pacific plate (Figure 14). An additional parameter (Explorer-Pacific motion rate, or Explorer-North America motion or motion direction) is needed to close the triangle. A less northerly orientation of the Pacific-Explorer motion relative to the Pacific-North America motion, well constrained by the slip vector azimuths, requires some convergence between the Explorer and North American plates. We closed the triangle by choosing Explorer-North America motion perpendicular to Explorer-Pacific motion (gray lines, Figure 14). This choice minimizes Explorer-North America motion at the triple junction (0.7 cm/yr). The Explorer-North America motion direction (azimuth of 65°) is not perpendicular to the North American margin (trend about 325°); the model, thus, predicts a small component of left-lateral Explorer-North America motion (0.1 cm/yr) besides the more prominent component of convergent motion (0.6 cm/yr). The choice fixes the Pacific-Explorer motion rate at the triple junction to 4.5 cm/yr, which is equivalent to a Pacific-Explorer rotation rate of 3.3°/Myr (Table 3). Requiring purely convergent Explorer-North America motion at the triple junction (azimuth 55°, rate 0.7 cm/yr) changes the Pacific-Explorer motion rate only slightly to 4.4 cm/yr (and the Pacific-Explorer rotation rate to 3.2°/Myr). Other choices of Explorer-North America motion result in similar Pacific-Explorer rotation rate estimates.

[49] The North America-Explorer, Juan de Fuca-Explorer, and Hotspot-Explorer rotation poles (Table 3 and Figure 12) are obtained by vector addition of the Pacific-Explorer pole with other published poles [*Wilson*, 1993; *DeMets et al.*, 1994; *Gripp and Gordon*, 1990]. According to model A (gray arrows, Figure 15), Explorer-North America motion is predominantly convergent and the rate increases from about 0.7 cm/yr near the Tuzo Wilson seamounts (in a direction of 65°) to about 2.2 cm/yr off Nootka Island (azimuth 53°); right-lateral Explorer-Pacific motion changes only little from the northwest part of Revere-Dellwood-Wilson fault (rate 4.5 cm/yr, azimuth 155°) to the Southwest Explorer transform(s) (rate 4.9 cm/yr, azimuth 140°), and left lateral motion along Nootka fault has a rate of about 2.4 cm/yr. The predicted motion direction along the southwestern part of Nootka fault (azimuth of about 55°), however, does not agree with observed slip vector azimuths (average of 37°).

4.2. Pacific-Explorer Rotation Pole, Model B

[50] In model B, we included slip vector azimuths from the southwest part of Nootka fault (region 9, Tables 1 and 2,

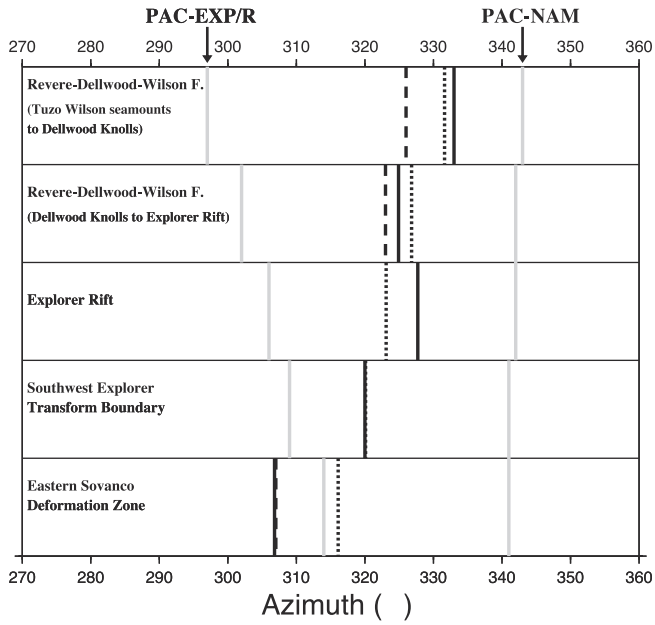

Figure 13. Pacific-Explorer motion directions predicted by model A's Pacific-Explorer rotation pole (dotted). Model B's predicted directions (not shown) are similar. Panels are the same as in Figure 6. For each panel, the solid line is the average observed slip vector azimuth, the dashed line is the active fault trend, and the gray lines are Pacific-North America (PAC-NAM, from NUVEL-1 [*DeMets et al.*, 1990]) and *Riddihough*'s [1984] Pacific-Explorer (PAC-EXP/R) motion directions. For the top four panels, note the good agreement between predicted motion direction and observations (average slip vector azimuth and bathymetry). For the ESDZ, note the large discrepancy between predicted motion direction and observations; aseismic motion on the conjugate faults may account for this discrepancy.

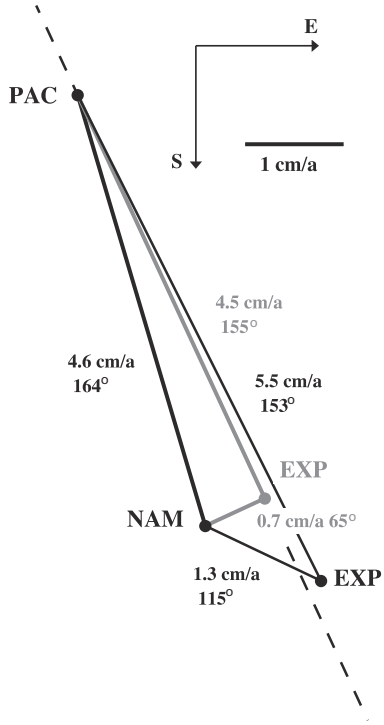

Figure 14. Velocity triangle at the Pacific-North America-Explorer (PAC-NAM-EXP) triple junction near the Tuzo Wilson seamounts. For model A, PAC-NAM motion (black line, NUVEL-1A [*DeMets et al.*, 1994]) and PAC-EXP motion direction (black dashes) are defined. We close the triangle by minimizing EXP-NAM motion (0.7 cm/yr in a 65° direction, gray line). The resulting EXP-PAC motion rate (4.5 cm/yr in a 155° direction, gray line) is equivalent to a rotation rate of 3.3°/Myr (for PAC-EXP pole at 54.0°N, 120.0°W, Figure 12 and Table 3). For model B, rotation rate (3.1°/Myr) and location (54.8°N/116.6°W) of the PAC-EXP pole are determined simultaneously with slip vector data from the PAC-EXP and the Juan de Fuca-EXP boundaries. Predicted EXP-NAM (1.3 cm/yr in a 115° direction) and EXP-PAC (5.5 cm/yr in a 153° direction) motions are shown as thin solid lines.

excluding three events near Nootka Island, which possibly did not occur on Nootka fault) to find a Pacific-Explorer rotation pole, which is consistent with observations along the Pacific-Explorer and the Explorer-Juan de Fuca plate boundaries. With slip vector azimuths from two plate boundaries and a known Pacific-Juan de Fuca rotation pole (we used the pole given by *Wilson* [1993]), the location and rate of the Pacific-Explorer rotation pole can be determined.

[51] We extended the grid search to include rotation rate as a parameter. For each trial Pacific-Explorer rotation pole, we calculated an Explorer-Juan de Fuca rotation pole by vector addition of the trial Pacific-Explorer to *Wilson*'s [1993] Pacific-Juan de Fuca rotation pole. A Pacific-Explorer pole at 54.8°N, 116.6°W rotating with a rate of 3.1°/Myr fits the observed slip vector azimuths along both plate boundaries best in a least squares sense. The Pacific-Explorer pole location is mainly determined by observations from the Pacific-Explorer boundary, where we have about five times as many slip vectors compared to the Explorer-Juan de Fuca boundary. The pole's location uncertainty and the predicted Pacific-Explorer motion directions are similar to model A (and thus not shown in Figures 12 and 13). For a given Pacific-Explorer pole location, the Explorer-Juan de Fuca slip vector azimuths constrain the Pacific-Explorer rotation rate tightly. For example at the best fitting Pacific-Explorer pole location, the rate changes only by ±0.2°/Myr for a misfit increase of 3%. The North America-, Juan de Fuca-, and Hotspot-Explorer rotation poles are listed in Table 3 and shown in Figure 12.

[52] Model B (black arrows, Figure 15) predicts 5.5–6 cm/yr right-lateral Pacific-Explorer motion, oblique convergence between the Explorer and North American plates (with the rate increasing from about 1.3 cm/yr of predominantly left-lateral motion near the Tuzo Wilson seamounts to about 2.2 cm/yr of equal left-lateral and convergent motion offshore Nootka Island), and about 2.5 cm/yr left-lateral motion along Nootka fault. The predicted Explorer-Juan de Fuca relative motion trend (azimuth 35°–40°) agrees well with the slip vector azimuths along Nootka fault. The main differences compared to model A are (Figures 14 and 15): Pacific-Explorer motion rate is faster; Explorer-North America motion, though similar in rate along most of the plate boundary, has a strong left-lateral component and is much more oblique, and Explorer-Juan de

Table 3. Instantaneous Rotation Poles of Explorer Plate[a]

Plate Pair	Latitude, °N	Longitude, °W	ω deg/Myr	ω_x, deg/Myr	ω_y, deg/Myr	ω_z, deg/Myr	Comment
			Model A				
PAC-EXP	53.99	120.04	3.30	−0.9701	−1.6775	2.6662	
JDF-EXP	45.92	125.76	3.37	−1.3694	−1.9016	2.4197	W′93
NAM-EXP	52.67	131.90	2.65	−1.0714	−1.1940	2.1037	N-1A
HSP-EXP	49.81	129.12	2.38	−0.9698	−1.1927	1.8199	HS2
			Model B				
PAC-EXP	54.80	−116.62	3.10	−0.8007	−1.5975	2.5332	
JDF-EXP	46.35	−123.38	3.16	−1.2000	−1.8216	2.2866	W′93
NAM-EXP	53.97	−129.00	2.44	−0.9020	−1.1140	1.9707	N-1A
HSP-EXP	50.90	−125.73	2.17	−0.8004	−1.1127	1.6869	HS2

[a]PAC-EXP, Pacific-Explorer rotation pole derived in this study. Second (EXP) plate moves relative to first (PAC) plate, positive rotation rate ω indicates counterclockwise rotation; ω_x, ω_y, ω_z are Cartesian coordinates of rotation vector. Plate abbreviations are EXP, Explorer; PAC, Pacific; JDF, Juan de Fuca; NAM, North America; HSP, hot spot reference frame. W'93, vector addition of PAC-EXP pole with PAC-JDF pole from *Wilson* [1993]. N-1A, vector addition with NUVEL-1A PAC-NAM pole from *DeMets et al.* [1994]. HS2: vector addition with PAC-HSP pole from *Gripp and Gordon* [1990].

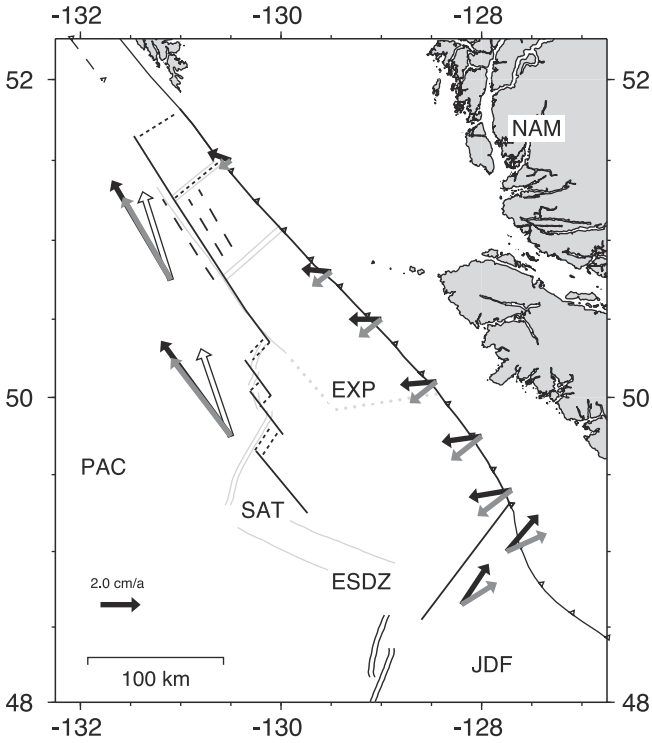

Figure 15. Present-day Explorer plate motions (model A is gray arrows and model B is black arrows; open arrows are Pacific-North America motion vectors [*DeMets et al.*, 1994]). Arrows point in the direction the surrounding plates move relative to Explorer plate. Explorer plate's boundaries are shown in heavy black (transforms are solid lines, long dashes where inferred; subduction zone is barbed line; short dashes are spreading centers or extensional pull-apart basins). We infer the extent of the Eastern Sovanco Deformation Zone (ESDZ) from the earthquake distribution (Figure 9). The Southwestern Assimilated Territory (SAT) was recently transferred from the Explorer to the Pacific plate; the SAT is bordered to the northeast by one or several Pacific-Explorer transform faults. Light gray lines show plate boundaries from Figure 1.

Fuca motion is more northerly oriented, which is required by the Nootka slip vector azimuths used to derive model B.

4.3. Seismic Slip Rates

[53] We estimated seismic slip rates for six segments (Revere-Dellwood-Wilson, Explorer Rift, Explorer Deep, Southwest Explorer boundary, ESDZ, and Nootka fault) to see how much of the predicted plate motions is taken up seismically. The seismic slip rates are based on 80 years of seismicity and include corrections for location and magnitude bias (Appendix C). The estimates, probably good to within a factor of 2, are listed in Table C1.

[54] The estimated seismic rates are not useful in distinguishing between the plate models (model A or B) because of the large seismic slip rate uncertainties and the unknown, and probably varying, ratio of seismic-to-aseismic energy release between different segments. The seismic rates, however, show that about half of the predicted Pacific-Explorer plate motion (model A, 4.5 cm/yr; model B, 6.0 cm/yr) is released seismically in large earthquakes along the Revere-Dellwood-Wilson (seismic rate of 3.4 cm/yr) and Southwest Explorer (2.4 cm/yr) transform segments. For these two segments, earthquakes of magnitude greater than 5.5 account for almost all of the observed seismic rates. In comparison, along the Explorer Rift segment, the seismic rate is only 0.6 cm/yr, and larger earthquakes contribute only two thirds of the seismic rate. The small lengths of the transforms associated with the Explorer Rift and presumably, warmer, thinner crust may account for these characteristics. Along the ESDZ, the seismic rate is 2.0 cm/yr (assuming motion along one fault) and the contribution of large events is similar to the Revere-Dellwood-Wilson and Southwest Explorer transform segments. Because earthquakes account for a substantial part of the Pacific-Explorer relative motion, we feel seismicity provides an accurate view of the present-day motions along this boundary.

[55] The predicted rate along Nootka fault is about 2.5 cm/yr for both models A and B. The seismic rate estimate is 0.3 cm/yr. If the large 1918, M_S = 7.2 event that *Cassidy et al.* [1988] located on Vancouver Island is included, the rate would increase to 1.5 cm/yr. The lower estimate indicates that earthquakes along Nootka fault contribute less to the plate motions than those along the Pacific-Explorer transform segments, or alternatively, seismicity along Nootka fault has been unusually low during the last 80 years.

5. Discussion

5.1. Tectonic Model of Explorer Plate for the Last 3 Myr

[56] Motions of the Explorer plate, since its inception about 4 Ma, are characterized by successive clockwise rotation of the Explorer ridge system and the Explorer-Pacific transform boundaries. Rotation brings the Explorer ridge system closer to being perpendicular to the North American plate boundary and causes the Explorer-Pacific transform faults to become oriented increasingly more parallel to the southern end of the Queen Charlotte fault. This reorganization reduces relative motion between the Explorer and North American plates. Before separation of Explorer plate from the Juan de Fuca plate about 4 Ma, Juan de Fuca plate subducted at a rate greater than 5 cm/yr beneath North America, while Juan de Fuca-Pacific motion was close to east-west (azimuth of 105° at 50°N, 130°W) [*Riddihough*, 1984]. After the plate breakup, the relative motion of the new established Explorer plate with respect to North America was slower (about 3–4 cm/yr) and the direction of motion with respect to the Pacific plate had shifted clockwise to an azimuth of about 120° [*Riddihough*, 1984]. The current maximum Explorer-North America motion rate is about 2 cm/yr and the Explorer plate moves in a southeasterly direction (average azimuth of about 145°) relative to the Pacific plate (Figure 15).

[57] Explorer plate, at the time of plate breakup, constituted the youngest part of the Juan de Fuca plate. Resistance of young, buoyant material to subduct beneath North America has been cited as a potential reason for the breakup [*Riddihough*, 1984]. After the plate breakup, the entire Explorer plate consisted of young (<10 Ma), buoyant oceanic crust. Moreover, only a short segment of subducting slab, from Brooks peninsula to the intersection of Nootka fault with the North American continental margin, existed to

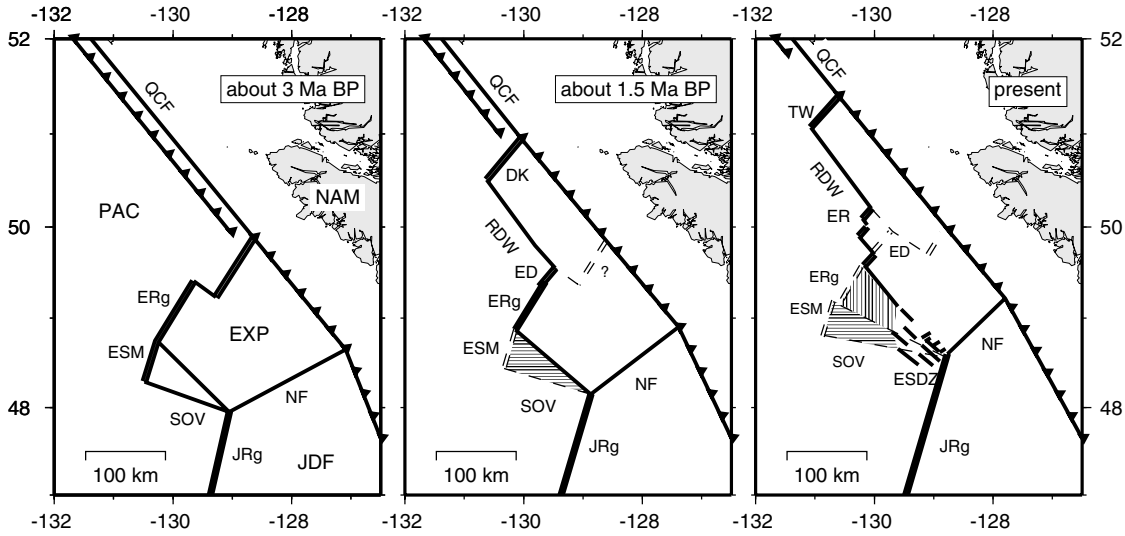

Figure 16. Schematic plate tectonic reconstruction of Explorer region during the last 3 Myr. Note the transfer of crustal blocks (hatched) from the Explorer to the Pacific plate; horizontal hatch indicates transfer before 1.5 Ma and vertical hatch transfer since then. Active boundaries are shown in bold and inactive boundaries are thin dashes. Single lines are transform faults, double lines are spreading centers; barbed lines are subduction zones with barbs in downgoing plate direction. QCF is Queen Charlotte fault, TW are the Tuzo Wilson seamounts, RDW is Revere-Dellwood-Wilson fault, DK are the Dellwood Knolls, ED is Explorer Deep, ER is Explorer Rift, ERg is Explorer Ridge, ESM is Explorer Seamount, SOV is Sovanco fracture zone, ESDZ is Eastern Sovanco Deformation Zone, JRg is Juan de Fuca ridge, and NF is Nootka fault. The question mark indicates ambiguity whether spreading offshore Brooks peninsula ceased when the Dellwood Knolls became active (requiring only one independently moving plate) or if both spreading centers, for a short time span, where active simultaneously (requiring Winona block motion independent from Explorer plate during that time).

provide slab pull forces. The reduction in slab-pull forces [e.g., *Forsyth and Uyeda*, 1975; *Turcotte and Schubert*, 1982], may have contributed to the slow-down of Explorer-North America motion.

[58] Figure 16 sketches the development of Explorer plate and its motions for three time steps (approximately 3 Ma, 1.5 Ma, and now). Since its inception, Explorer plate has undergone many adjustments in its configuration; each sketch, thus, represents a snapshot in a rather complicated development. Figure 16 builds on published tectonic models based primarily on interpretation of magnetic anomalies [*Riddihough*, 1977, 1984; *Riddihough et al.*, 1980; *Davis and Riddihough*, 1982; *Botros and Johnson*, 1988; *Lister*, 1989; *Wilson*, 1993] and our model for the present-day tectonics based on earthquake slip vectors and seismicity (Figure 15). Conceptually, our model of present-day tectonics is similar to a later stage of development for the Explorer plate system proposed by *Lister* [1989]. According to *Lister* [1989], a series of southward propagating ridges, each originating at the continental margin and each being rotated slightly clockwise relative to the previous propagator, successively changed the Explorer plate motions reducing the subduction rate relative to North America. At the present, Winona block and Explorer plate form one entity.

5.1.1. Around 3 Ma

[59] Around 3 Ma, Explorer plate moves independently of the Juan de Fuca plate. The Pacific-Explorer-North America triple junction is located offshore Brooks peninsula [*Riddihough*, 1977; *Lewis et al.*, 1997], and a short left-lateral transform connects the ridge segment offshore Brooks peninsula with Explorer ridge. Asymmetric spreading of Explorer ridge, where more material is accreted to the Explorer than to the Pacific plate, lengthens the transform [*Riddihough et al.*, 1980; *Davis and Riddihough*, 1982]. The Explorer ridge trends at an angle of about 28°, while its southern extension, the Explorer Seamount, shows an overall bathymetric trend of about 17° [*Botros and Johnson*, 1988]. The seamount is active at least until about 2.6 Ma (magnetic anomaly chron 2A) [*Botros and Johnson*, 1988]; its trend, however, remains parallel to Juan de Fuca ridge (roughly 20° during the last 4 Myr [*Riddihough*, 1984; *Botros and Johnson*, 1988]). After the Juan de Fuca plate breakup, Explorer Ridge rotates 10° clockwise, the seamount, however, remains in its original orientation. The Sovanco fracture zone connects Explorer Seamount with the Juan de Fuca Ridge. A triangular-shaped fracture/deformation zone may in fact be composed of two transform faults [*Lister*, 1989]. This configuration allows westward asymmetric spreading at the Explorer Seamount. The Nootka fault zone separates the Explorer plate from the Juan de Fuca plate. Its exact location and trend are not known, however, the fault zone, shown in the sketch, is consistent with estimates provided by *Hyndman et al.* [1979] and *Riddihough* [1984].

5.1.2. About 1.5 Ma

[60] About 1.5 Ma, Explorer plate's aerial extent and motion had changed considerably. Explorer-Pacific relative

motions are now defined by the incipient Revere-Dellwood fault trending at an angle of 315°–325°, which is equivalent to a 15°–25° clockwise rotation relative to prevalent Explorer-Pacific plate motion direction about 3 Ma.

[61] Spreading had jumped from offshore Brooks peninsula to the Dellwood Knolls. Onset of Dellwood Knolls volcanism, and thus timing of the ridge jump, is not known precisely. But uplift of the Paul Revere ridge, subsidence of the Winona basin and compression of sediments inside Winona basin beginning near the Pliocene-Pleistocene boundary (about 1.8 Ma) [*Kulm et al.*, 1973; *Davis and Riddihough*, 1982] are possibly a result of the ridge jump. *Riddihough et al.* [1980], who prefer a younger age for the Dellwood Knolls, cannot exclude a 1.5 Ma-or-older age of the knolls because of relatively thick manganese encrustation found in dredged basalts. The newly initiated right-lateral Revere-Dellwood (-Wilson) transform fault connects the Dellwood Knolls with the north tip of Explorer ridge; the fault east of Explorer ridge is now inactive.

[62] Winona basin, bordered by the Dellwood Knolls, the Revere-Dellwood fault and its inactive southeast extension, the inactive spreading center offshore Brooks peninsula, and the continental margin, has switched from the Pacific to the Explorer plate. The boundary between Winona basin and North America, which was a transcurrent boundary before the ridge jump, becomes a purely convergent margin. Depending on the exact timing of the ridge jump, Winona basin could have initiated as an independent microplate [*Davis and Riddihough*, 1982].

[63] Explorer-Pacific plate motions are defined by the Revere-Dellwood fault trend, which changes from about 325° near the Dellwood Knolls to about 315° close to its intersection with Explorer Deep. These directions are rotated clockwise by about 15°–25° relative to the Explorer-Pacific motions at the Explorer ridge and even more severely by 25°–35° at the Explorer Seamount (assuming ridge perpendicular spreading). The clockwise plate motion change may have caused cessation of volcanism at the Explorer Seamounts, which was inactive by chron 2 age (about 1.9 Ma) [*Botros and Johnson*, 1988]. Explorer spreading then terminates at the Explorer ridge's southern tip requiring a clockwise rotation of the Sovanco fracture zone to connect the Explorer and Juan de Fuca ridges.

5.1.3. Present-Day Explorer Plate

[64] The Revere-Dellwood-Wilson fault has lengthened to the northwest and now forms the Explorer-Pacific plate boundary from the Tuzo Wilson seamounts to the Explorer Rift. The fault trend of about 325° defines the current Explorer-Pacific plate motion direction. The Tuzo Wilson seamounts are now active and volcanism at the Dellwood Knolls has probably ceased. Considering our estimated Explorer-Pacific plate motion rates of 4.5–6.0 cm/yr, the distance of about 80 km between the two structures requires asymmetric spreading with more material accreting to the Explorer than to the Pacific plate; completely one-sided spreading can account for a distance of 45–60 km/Myr.

[65] Spreading jumped about 40 km to the northwest from the Explorer Deep to the Explorer Rift, probably, during the last 0.3 Myr [*Botros and Johnson*, 1988]. The ridge jump possibly was caused by misalignment of the Revere-Dellwood fault segment between Explorer Rift and Explorer Deep. The now inactive fault segment was less northerly oriented (about 315°) than the segment northwest of Explorer Rift (about 325°); the misalignment possibly also caused (part of) Paul Revere ridge uplift. The northern Explorer Rift spreading center abutting the Revere-Dellwood-Wilson fault is oriented at 42°, whereas Explorer Deep has a slightly more northerly trend of 36°. The difference is small, but the clockwise rotation of the spreading ridge centers from the inactive to the active agrees well with our model.

[66] Our earthquake distribution (Figure 9) suggests a new plate boundary, the Southwest Explorer Transform Boundary (SETB), intersects with Explorer ridge near 49.7°N. Thus only the northernmost part of the Explorer ridge is still actively spreading. The SETB possibly consists of several fault strands (Figure 9) and runs southeast (trend of about 140°) toward an ill-defined boundary with the ESDZ. Development of the SETB caused the transfer of a triangular shaped region from the Explorer to the Pacific plate; the region is bounded by the southern Explorer ridge, the western Sovanco fracture zone and SETB. In this respect, the SETB is similar to the southern part of the transform boundary proposed by *Rohr and Furlong* [1995].

[67] The tectonic development along the Explorer ridge and Explorer seamount system outlined in Figure 16, a more or less continuous northward retreat of spreading center activity during the last 3 Myr, represents a simplified picture. Continuity of Explorer ridge [see *Davis and Currie*, 1993, Figure 4] and continuity of the Brunhes magnetic anomaly (<0.7 Myr) south to about 49.2° [*Botros and Johnson*, 1988] requires transfer of the Explorer plate fragment to the Pacific plate occurred only recently. A transferred ridge segment would move with the Explorer-Pacific half-spreading rate of about 2–3 cm/yr (20–30 km/Myr) relative to the active ridge segment and ridge continuity would be destroyed within a short time span. However, a small ridge offset could be masked by a 5–10 km eastward jump of Explorer ridge during Brunhes anomaly [*Botros and Johnson*, 1988; *Michael et al.*, 1989] and by subcrustal, lateral magma flow from the active northern to the southern distal end of the ridge [*Michael et al.*, 1989].

[68] The width of the Brunhes anomaly along Explorer ridge narrows toward the south. *Botros and Johnson* [1988] interpret the narrowing in terms of southward propagation of Explorer ridge during the Brunhes anomaly. A southward propagating Explorer ridge would have required a phase of counter-clockwise rotation of Sovanco fracture zone, which could have contributed further to its broad, broken-up shear zone character. Currently, broadly distributed deformation is confined to the ESDZ, which forms the southeastern part of the Explorer-Pacific plate boundary. The ESDZ consists of elevated blocks bounded by conjugate faults. The northeast trending faults are primarily active based on fault trend orientations and slip vector azimuths (Figure 10). The slip vector azimuths, though, are about 10° less northerly than expected for Explorer-Pacific motion (Figure 13). Accommodation of all present-day Explorer-Pacific motion within the ESDZ, thus, requires a small amount of compensation, possibly by left-lateral motion along the northwest trending conjugate faults.

[69] We envision that the recently formed (or still forming) SETB could lengthen toward the southeast, eventually cutting through the ESDZ and forming a transform boundary between the Explorer and Juan de Fuca Ridges. Such a scenario would simplify the Explorer-Pacific plate boundary. The resulting boundary would consist primarily of two long transform segments (Revere-Dellwood-Wilson and Southwest Explorer Transform Boundary) separated by a step over consisting of short ridge-transform segments near Explorer Rift, and an extensional plate boundary near the Tuzo Wilson seamounts.

5.2. Explorer-North America Motion

[70] Both plate models presented predict convergent motion between the Explorer and North American plates increasing from about 0.5 cm/yr near the Tuzo Wilson seamounts to about 2 cm/yr near Nootka Island (Figure 15). Their common boundary, with the exception of events beneath Brooks peninsula, lacks earthquakes at the magnitude level greater than 4 (Figure 8). Sporadic, low-magnitude seismicity is, however, present (available at www.pgc.nrcan.gc.ca). A low seismicity rate along a convergent margin, however, is not entirely unusual; the margin of the Juan de Fuca and North America plates (the Cascadia subduction zone), for example, is also mostly aseismic in spite of a much faster convergence rate. Presumably, the convergence at the Cascadia subduction zone is taken up by infrequent (greater than 200-year recurrence cycles) megathrust earthquakes.

[71] In principle, the North American-Explorer convergence could be taken up by crustal thickening over a broad zone within the continent. However, GPS measurements from northern Vancouver Island show only minimal (less than 3 mm/yr) motions relative to stable North America (Pentincton) [*Dragert and Hyndman*, 1995]; hence no substantial convergence can be taken up on land east of Vancouver Island, and the convergence must be taken up offshore, most likely by subduction.

[72] The earthquakes beneath Brooks peninsula (Figure 11) probably occurred within the overriding North American crust. Their source mechanisms are quite unusual and indicate strike-slip motion on shallow-dipping, east-west striking fault planes (identified by aftershocks) [*Spindler et al.*, 1997]. *Spindler et al.* [1997] point out that the events' northeast-directed pressure axes, roughly parallel to Explorer-North America motion direction predicted by our model A, are consistent with stresses expected in the upper crust in a locked, or partially locked, subduction zone. Our model B predicts east-west oriented Explorer-North America motion, roughly parallel to the slip vectors of these earthquakes.

[73] The source mechanisms near Nootka Island are more similar to the mechanisms of the Brooks peninsula earthquakes than to the source mechanisms along southwestern Nootka fault. The Nootka Island events might thus represent Explorer-North America interaction.

[74] Other evidence supports active Explorer-North America convergence along the continental margin. The margin morphology changes significantly offshore Brooks peninsula, possibly the result of a long-lived ridge-transform-trench triple junction offshore Brooks peninsula [*Riddihough*, 1977; *Lewis et al.*, 1997]. Southeast of the peninsula, the continental margin is broad and deformed [*Tiffin et al.*, 1972; *Chase et al.*, 1975; *Davis and Hyndman*, 1989]; oceanic basement dips landward [*Davis and Hyndman*, 1989; *Clowes et al.*, 1997], and receiver function analysis, heat flow and gravity data reveal a subducting slab beneath Vancouver Island [*Cassidy et al.*, 1998; *Lewis et al.*, 1997].

[75] Northwest of Brooks peninsula, convergent motion began less than 2 Myr ago [*Riddihough et al.*, 1980; *Davis and Riddihough*, 1984]. The recent onset and small rate (<1.5 cm/yr, according to our plate models) limit overall convergence to less than 30 km, explaining the lack of a subducted slab beneath northern Vancouver Island [*Cassidy et al.*, 1998]. The margin's narrow, steep morphology [*Tiffin et al.*, 1972; *Chase et al.*, 1975] is probably a remnant of long-lived transform motion [*Lewis et al.*, 1997]. Evidence for convergence is found only in the Pleistocene Winona basin (the part of Winona Block southeast of the Dellwood Knolls, Figure 1), which is characterized by actively deforming, northwest striking compressional folds and ridges [*Srivastava et al.*, 1971; *Chase et al.*, 1975; *Davis and Riddihough*, 1982]. Progressively increasing sediment deformation from northwest to southeast inside the basin [*Srivastava et al.*, 1971; *Riddihough et al.*, 1980; *Davis and Riddihough*, 1982] is consistent with our plate models, which predict a northwest to southeast increase in Explorer-North America motion (Figure 15). Seismic data and gravity modeling [*Yuan et al.*, 1992] are consistent with active subduction.

[76] Model A places the North America-Explorer rotation pole on the southern Queen Charlotte Islands (Figure 12). This implies that the region between Dellwood Knolls southern Queen Charlotte Islands, even if part of the Explorer plate system, should exhibit only minimal motion relative to North America. The earthquakes there should represent primarily Pacific-North America interaction. Southeast of Queen Charlotte Islands, the morphological expression of the terrace paralleling the Queen Charlotte fault and any other geological expression of slip partitioning (convergence) rapidly disappear. In absence of slip partitioning, earthquake slip vectors in this region should parallel the expected Pacific-North America motion. This is indeed the case; the average slip vector for events on the Revere-Dellwood-Wilson extension northwest of the Tuzo Wilson seamounts and the southern most event on the Queen Charlotte fault has exactly the trend of predicted Pacific-North America motion (344°).

5.3. Southwest Assimilated Territory: Capture of a Microplate Fragment

[77] An interesting result is the proposed transfer of a large Explorer plate fragment (the SAT) to the Pacific plate in the southwest corner of the Explorer region (Figure 16). The material transfer is a result of clockwise rotation of Explorer motions relative to the Pacific plate requiring a reorientation of the Explorer-Pacific plate boundary. The triangular-shaped SAT extends roughly from 48.6°N to 49.7°N and from 130.7°W to 129.7°W, its northeastern boundary is the SETB defined by seismicity (Figure 9). Capture of the SAT probably did not happen in one episode. As mentioned before, Explorer plate motions appear to have changed steadily and the part of the SAT east of the Explorer

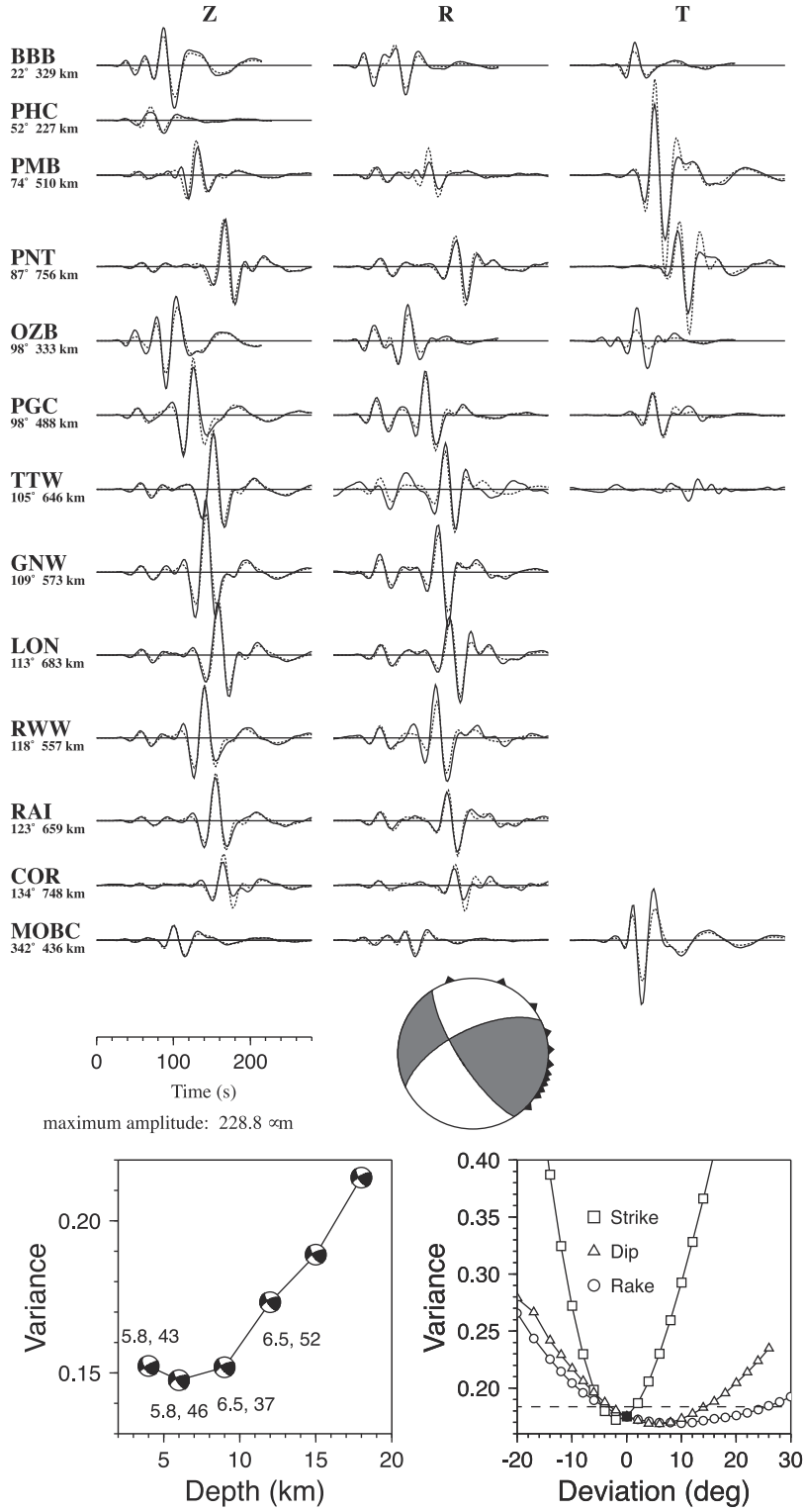

Figure A1. (top) Observed (solid) and synthetic (dashed) seismograms for the best fit model in the 25-to 100-s period passband for the 0712 UTC, 9 October 1996 M_w = 5.8 earthquake. Z, R, and T are vertical, radial, and transverse components. All seismogram amplitudes are normalized to an epicentral distance of 100 km assuming cylindrical geometrical spreading. The stations are listed in azimuthal order with numbers beneath station codes giving event-station azimuth and distance. The triangles on the fault plane solution (lower hemisphere projection) depict the station azimuthal coverage. (bottom left) Residual variance reduction versus centroid depth. Numbers beneath the fault plane solutions are seismic moment (in 10^{17} N m) and percent double couple of moment tensor solution. (bottom right) Residual variance reduction versus deviation from best fitting double-couple mechanism for 6 km centroid depth and northwest trending fault. The dashed line represents a 5% variance increase relative to best fit double couple.

Seamount was probably captured about 2 Ma, while the area east of Southern Explorer Ridge transferred only recently. Magnetic anomalies inside the SAT are distorted [see *Botros and Johnson*, 1988, Figure 4]; and later recognition of capture would mainly depend on identifying the preserved former Explorer-Pacific ridge (Explorer Seamount and south part of Explorer ridge) now moving within the Pacific plate. The capture of the SAT, caused by the clockwise rotation of the Explorer Ridge and the Sovanco transform systems, is ultimately caused by the difficulty of subducting young oceanic crust. Such capture, although quite different in geometric details, has been also reported for microplate fragments offshore California and Baja California [*Atwater*, 1989; *Lonsdale*, 1991; *Stock and Lee*, 1994; *Nicholson et al.*, 1994; *Bohannon and Parsons*, 1995].

6. Summary and Conclusions

[78] The new seismological data presented in this study, consisting of reliable, waveform modeling derived moment tensor solutions and JED earthquake relocations, constrain the current tectonics of the Explorer region. The earthquake slip vector azimuths along the Pacific boundary vary smoothly and are less northerly oriented than Pacific-North America plate motion. This observation requires the existence of an independent Explorer plate.

[79] The current Explorer-Pacific boundary, well defined by seismicity, is formed by the Revere-Dellwood-Wilson and subparallel transform faults, which are offset by short right-stepping spreading segments. The faults are more northerly oriented than motion directions frozen into older (about 2 Ma) magnetic anomaly data requiring a recent plate motion re-orientation. It appears that the current Explorer plate motions are the result of successive clockwise rotations of the Explorer ridge system; each rotation brought the ridges closer to being perpendicular to the continental margin and thus reduced convergent Explorer-North America plate motions. As response to these plate motion changes, a region encompassing the western Sovanco fracture zone appears to be in the process of being transferred from the Explorer to the Pacific plate.

[80] A region near the eastern Sovanco fracture zone is characterized by a broadly distributed seismicity. The region is composed of elevated blocks bounded by conjugate faults. Earthquake slip vectors indicate the northwest trending faults are primarily active. The slip vectors, however, are less northerly oriented than the current Explorer-Pacific motion requiring some left-lateral motion, possibly along the conjugate faults, to fully accommodate all present-day motions.

[81] Nootka fault is a left-lateral transform fault forming the Explorer-Juan de Fuca plate boundary. Its full extent under Nootka Island remains unresolved, which leaves some ambiguity in the inference about Explorer plate's current motions.

[82] Our Explorer-North America pole of rotation predicts small convergence increasing from negligible to about 2 cm/yr from northwest to southeast along the Explorer-North America boundary. Southeast of Brooks peninsula, a well-established subduction zone exists and ongoing convergence is probably accommodated by subduction. The boundary segment between Brooks peninsula and the Tuzo Wilson seamounts became part of Explorer plate only during the last 0–2 Myr. Deformed sediments inside the Winona basin indicate ongoing convergence.

Table B1. Pre-1964 Earthquake Relocations in Explorer Region's Southwest Corner[a]

Date	Mag	Latitude, °N	Longitude, °W	NA	AzGp, deg
3509232212	6.2 PAS	49.45	128.89	22	210
3901031718	5.6 PAS	49.43	129.63	10	190
3902080539	6.5 EPB	48.88	128.06	9	194
3907180326	6.5 EPB	48.87	129.73	36	188
4110011949[b]	6.0 EPB	48.94	129.35	16	284
4206091106	5.7 EPB	49.63	129.06	9	194
4607180606	6.5 EPB	49.40	130.04	35	158
4607180716	6.5 EPB	49.32	129.93	29	158
6206021226	5.8 EPB	49.77	130.07	30	149

[a]Date is year month day hour minute. Mag is magnitude and source; PAS, Pasadena; EPB, Earth Physics Branch, Canadian Geological Survey, Ottawa. Latitude and longitude are relocated latitude and longitude. NA is number of arrival time picks used in relocation. AzGp is maximum azimuthal gap between two stations.

[b]Relocation using both regional and teleseismic *P* wave arrival time data. All other events were relocated using teleseismic data only.

Appendix A: Examples of Waveform Fits from RMT Analysis

[83] In this appendix and in electronic supporting Appendix D, we present examples of waveform fits and source parameter uncertainty estimates from regional moment tensor analysis for five earthquakes. For all five events both the RMT and CMT solutions are available. Double-couple orientations (strike/dip/rake) follow the convention of *Aki and Richards* [1980]. Centroid depths are given relative to the seafloor.

[84] We use the 9 October 1996 (0712 UTC; $M_0 = 5.77 \times 10^{17}$ N m, $M_w = 5.8$) earthquake located at the Southwest Explorer Transform Boundary to illustrate the quality of the observed regional waveforms, the theoretical wavefom fits and the resolution of derived earthquake source parameters. For this solution we employ 30 seimograms from 12 stations. The strike-slip source mechanism (147/75/153) for this event on a transform fault agrees with the CMT solution of 332/72/184. The source mechanism is constrained by the strong azimuthal amplitude variations of the waveforms. The waveform fit in the 0.01–0.04 Hz passband is generally good. Uncertainties in strike, dip, rake and centroid depth were estimated by observing the variance increase relative to the best fit model (lower right of Figure A1). The 6-km, shallow centroid depth is well resolved (lower left of Figure A1). For a northwest trending fault and 6 km centroid depth, we find strike more tightly constrained than dip and rake. The bounds for a 5% variance increase are ±4°, +15° to −5°, and +25° to −5° for strike, dip, and rake, respectively. A more rigorous statistical *t* test [*Huang et al.*, 1986], applied to all RMT solutions in the Explorer region, revealed that a 5% variance increase is commonly equivalent to a 75% to 90% confidence level. Additional examples are published in the electronic supplement.

Appendix B: Relocation of Pre-1964 Earthquakes

[85] In this appendix, we relocate large older earthquakes, which could have occurred in or near Explorer region's

Table C1. Seismic Slip Rates Versus Plate Motion Rates[a]

Segment	Length, 10^3 m	EV	LEV	$\sum (M_0)$, 10^{18} N m	LCO, %	Rate, mm/yr	Model A, mm/yr	Model B, mm/yr	R, mm/yr	WIL, mm/yr
RDW	150	202	30	141.5	97	34	46	56	44	
ER	50	67	13	8.4	67	6	47	57	42	
SWE	70	49	14	49.8	96	25	48	58	40	
ED	?	45	3	7.1	70	?				
ESDZ	80	107	20	37.9	90	17	49	59	39	
NOO	150	62	9	64.0	96	15	24	25	29	45
	150	61	8	13.9	83	3	24	25	29	45

[a]We assumed an uniform seismogenic width of 10 km, a rigidity of 3.5×10^{10} N/m^2, and 80 years of data coverage for each segment. Segment abbreviations are RDW for Revere-Dellwood-Wilson transform, ER for Explorer Rift, SWE for Southwest Explorer transform boundary, ED for Explorer Deep, ESDZ for Eastern Sovanco Deformation Zone, and NOO for Nootka transform. Length is the segment length. EV is the number of events. LEV is the number of $M \geq 5.5$ events. $\sum (M_0)$ is cumulative seismic moment. LCO is contribution of $M \geq 5.5$ events to cumulative seismic moment. Rate is estimated seismic slip rate. Model A, model B, R, WIL are predicted rates for plate model rate for model A, model B, *Riddihough* [1984], and *Wilson* [1993], respectively. See text for explanation for NOO segment.

southwest corner. We selected all $M \geq 6$ earthquakes that occurred from 1918 to 1963 and were listed by the International Seismological Summary, the Canadian Earth Physics Branch (EPB, now the Geological Survey of Canada (GSC)), or the *Gutenberg and Richter* [1954] catalogs to have occurred in the Explorer region south of 50°N and west of 129.5°W. The arrival time data are from the ISS. The teleseismic ($\Delta \geq 16°$) *P* wave arrival time data set is rather sparse. We thus relocated the historic earthquakes relative to the post-1963 events shown in Figure 7 with the JED technique. The station corrections were established by holding fixed the locations and origin-times of the more recent, generally better recorded events; this stabilized the relocation of the historic events. Earthquake depths were fixed to 10 km. Table B1 lists the relocated epicenters shown in Figure 9.

[86] For the events, which occurred during 1941, only stations in the United States and Canada reported arrival time data. This severely restricted the azimuthal coverage, thus degrading the location quality. For the 1 October 1941 event, we added regional picks to the teleseismic arrival time data to improve the azimuthal coverage; this helped to constrain the event's longitude (Figure 9 and Table B1). We could not reliably relocate the 6 November 1941 earthquake listed in the EPB catalog as an $M = 6$ event at 49.35°N and 129.83°W. For this event, most arrival times come from a narrow band of azimuths from stations in California, southeast of Explorer region, and a single pick from the College, Alaska, station to the northwest. This pick strongly affects the location estimate. With the College pick the epicenter is at about 49°N/130°W and without at 48°N/125°W. Because of the sensitivity of this event's location to a single arrival time pick, we decided not to use this event.

Appendix C: Seismic Slip Rate Estimates

[87] In this appendix, we compare seismic slip rates for several segments along Explorer region's plate boundaries with predicted plate motion rates to determine if earthquakes contribute significantly to the plate motions. Seismic slip rate of a fault is its cumulative seismic moment divided by fault area, material rigidity, and time span. We assumed a rigidity of 3.5×10^{10} N/m^2 and a uniformly 10-km-wide seismogenic layer based on the RMT centroid depth distri-

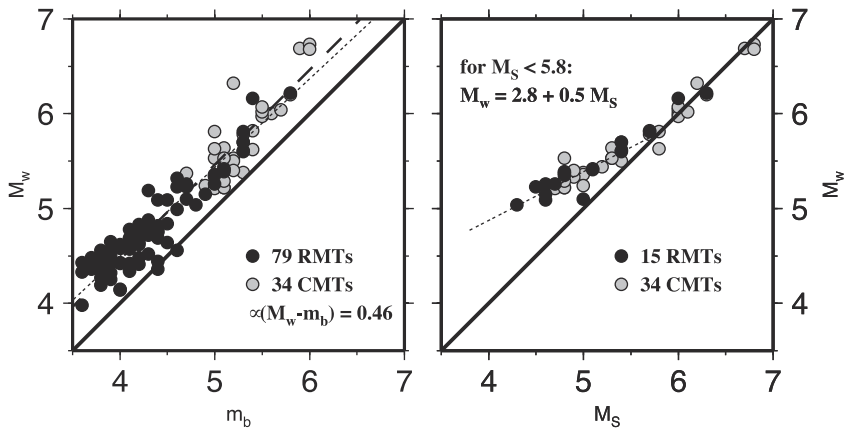

Figure C1. (left) Moment magnitude (M_w) versus body wave magnitude (m_b). (right) M_w versus surface wave magnitude (M_S). Black circles are regional moment tensor solutions (RMT) and gray circles are Harvard centroid moment tensor solutions (CMT). For a one-to-one correspondence between the magnitude scales, all circles would fall on the diagonal (solid black line). The M_w versus m_b figure indicates that on average M_w is 0.46 units bigger than m_b (long dashes); the least squares fit (short dashes) is only insignificantly different from the average difference. M_w versus M_S shows that for $M_S \geq 5.8$, M_w and M_S are equivalent; for $M_S < 5.8$, linear regression gives $M_w = 2.8 + 0.5\ M_S$ (short dashes).

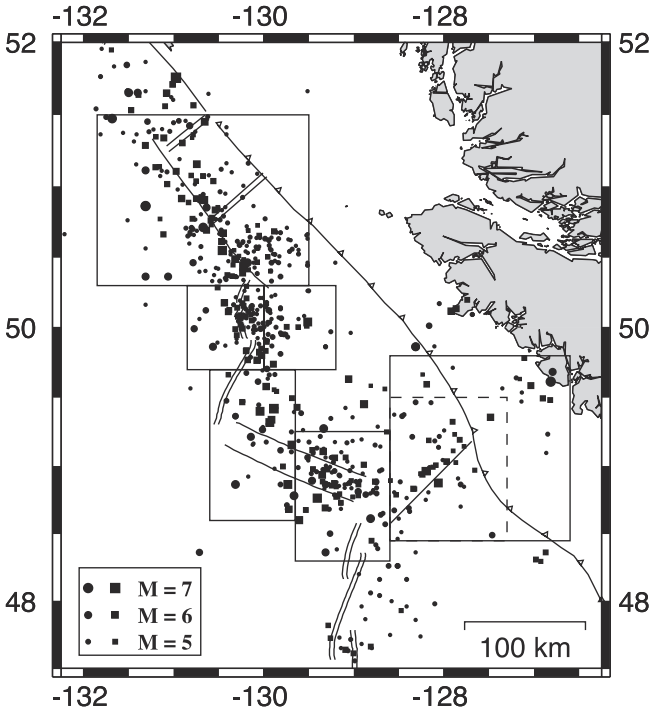

Figure C2. Magnitude ≥4.0 earthquakes in Explorer region (1912–1997) used for estimating seismic slip rate. ISC, PDE, GSC, and DNAG catalogs, and CMT and RMT solutions were used. We use relocated epicenters (squares) when available. For not relocated events (circles), we moved the epicenters by the average relocation bias (15 km to south, 22 km to west). We divided the Explorer plate boundary into six segments (Table C1) and assigned all events inside a box to that segment (see text for details on Nootka fault region).

bution (Figure 4). Segment lengths listed in Table C1 were estimated from bathymetry and seismicity (Figures 7–9).

[88] We added magnitude estimates from the ISC, PDE, EPB (now GSC), and the Decade of North American Geophysics (DNAG) catalogs covering the last 80 years to the moment tensors for the cumulative seismic moments. The catalogs provide only magnitude estimates that we converted to seismic moment using a moment-magnitude relationship [*Hanks and Kanamori*, 1979]. We first applied the relationship to events with a RMT or CMT solution to compare the moment magnitudes (M_w) with the body (m_b) and surface (M_S) wave magnitude estimates (Figure C1). For our data set, we found that an events' m_b is systematically smaller (on average by 0.46 magnitude units) than its M_w, and that M_S and M_w are equivalent only for $M_S \geq 5.8$. We thus added 0.46 magnitude units to m_b before applying the moment-magnitude relationship to the smaller catalog events ($M < 5.8$) and only converted larger events ($M \geq 5.8$) directly.

[89] We considered six segments: Revere-Dellwood-Wilson, Explorer Rift, Explorer Deep, north of western Sovanco, ESDZ, and Nootka. Assigning relocated events (Figure 7) was straightforward. For other events, we removed the average bias found from relocation (15 km south, 22 km west) before assigning events to a segment (Figure C2). The large number of $M \geq 4$ events (520) deemphasizes questionable assignments. The sizes of the selection boxes are appropriate considering large location errors for older events.

[90] The resulting estimates of slip rate (Table C1) agree well with *Hyndman and Weichert*'s [1983] results and imply that a large percentage of the predicted plate motions (Table C1) are accommodated seismically. Considering the effects introduced by erroneous assessments of fault area, rigidity and cumulative seismic moment (catalog completeness, segment assignment, magnitude-moment conversion, moment versus moment tensor summation), we suggest our seismic slip rates are good within a factor of 2, and random errors outweigh systematic errors greatly.

[91] Two estimates of seismic slip rate are listed for Nootka transform. The first and second assume the active fault extends beneath the North American margin to Nootka Island. The first estimate (1.5 cm/yr) is almost entirely dominated by one (6 December 1918) $M_S = 7.2$ earthquake beneath Nootka Island, which probably occurred above the transform in North American crust [*Cassidy et al.*, 1988]; excluding that event results in the second estimate (0.3 cm/yr).

[92] **Acknowledgments.** We thank A. Douglas for the JED program used in this study; J. Dewey for 1988 PDE phase arrival data; J. Cassidy, R. Horner, and G. Rogers of the Geological Survey of Canada at the Pacific Geoscience center for earthquake locations and broadband data from Vancouver Island; and R. Dziak and C. Fox at NOAA/PMEL for SOSUS earthquake locations. Other broadband waveform data were contributed by the Canadian Digital Seismic Network, Pacific Northwest Seismic Network, and U.S. National Seismic Network. B. Leitner participated in moment tensor determinations. We appreciate discussions with K. Rohr about the subject. Plots were generated using the GMT plotting software [*Wessel and Smith*, 1995]. The Swiss Seismological Service provided financial support to finalize the manuscript. We benefited from reviews by E. Davis, K. Furlong, and G. Rogers. This research was supported by the NSF grant OCE-9521929.

References

Aki, K., and P. G. Richards, *Quantitative Seismology: Theory and Methods*, vol. 1, W. H. Freeman, New York, 1980.

Allan, J. F., R. L. Chase, B. Cousens, P. J. Michael, M. P. Gorton, and S. D. Scott, The Tuzo Wilson volcanic field, NE Pacific: Alkaline volcanism at a complex, diffuse, transform-trench-ridge triple junction, *J. Geophys. Res.*, *98*, 22,367–22,387, 1993.

Atwater, T., Plate tectonic history of the northeast Pacific and western North America, in *The Geology of North America,* vol. N, *The Eastern Pacific Ocean and Hawaii*, edited by E. L. Winterer, D. M. Hussong, and R. E. Decker, pp. 21–72, Geol. Soc. of Am., Boulder, Colo., 1989.

Barr, S. M., and R. L. Chase, Geology of the northern end of the Juan de Fuca Ridge and sea-floor spreading, *Can. J. Earth Sci.*, *11*, 1384–1406, 1974.

Bérubé, J., G. C. Rogers, R. M. Ellis, and E. O. Hasselgren, A microseismicity study of the Queen Charlotte Islands region, *Can. J. Earth Sci.*, *26*, 2556–2566, 1989.

Bird, A. L., and G. C. Rogers, Earthquakes in the Queen Charlotte Islands region (abstract), *Eos Trans. AGU*, *77*(46), Fall Meet. Suppl., F522, 1996.

Bohannon, R. G., and T. Parsons, Tectonic implications of post-30 Ma Pacific and North America relative plate motions, *Geol. Soc. Am. Bull.*, *107*, 937–959, 1995.

Botros, M., and H. P. Johnson, Tectonic evolution of the Explorer-northern Juan de Fuca region from 8 Ma to the present, *J. Geophys. Res.*, *93*, 10,421–10,437, 1988.

Bouchon, M., The complete synthesis of seismic crustal phases at regional distances, *J. Geophys. Res.*, *87*, 1735–1741, 1982.

Braunmiller, J., J. L. Nábělek, B. Leitner, and A. Qamar, The 1993 Klamath Falls, Oregon, earthquake sequence: Source mechanisms from regional data, *Geophys. Res. Lett.*, *22*, 105–108, 1995.

Carbotte, S. M., J. M. Dixon, E. Farrar, E. E. Davis, and R. P. Riddihough,

Geological and geophysical characteristics of the Tuzo Wilson seamounts: Implications for the plate geometry in the vicinity of the Pacific-North America-Explorer triple junction, *Can. J. Earth Sci.*, *26*, 2365–2384, 1989.

Cassidy, J. F., and G. C. Rogers, The rupture process and aftershock distribution of the 6 April 1992 M_S 6.8 earthquake, offshore British Columbia, *Bull. Seismol. Soc. Am.*, *85*, 716–735, 1995.

Cassidy, J. F., R. M. Ellis, and G. C. Rogers, The 1918 and 1957 Vancouver Island earthquakes, *Bull. Seismol. Soc. Am.*, *78*, 617–635, 1988.

Cassidy, J. F., R. M. Ellis, C. Karavas, and G. C. Rogers, The northern limit of the subducted Juan de Fuca plate system, *J. Geophys. Res.*, *103*, 26,949–26,962, 1998.

Chase, R. L., D. L. Tiffin, and J. W. Murray, The western Canadian continental margin, in *Canada's Continental Margins and Offshore Petroleum Exploration*, edited by C. J. Yorath, E. R. Parker, and D. J. Glass, *Mem. Can. Soc. Pet. Geol.*, 4, 701–721, 1975.

Clowes, R. M., D. J. Baird, and S. A. Dehler, Crustal structure of the Cascadia subduction zone, southwestern British Columbia, from potential field and seismic studies, *Can. J. Earth Sci.*, *34*, 317–336, 1997.

Cousens, B. L., R. L. Chase, and J. G. Schilling, Basalt geochemistry of the Explorer Ridge area, northeast Pacific Ocean, *Can. J. Earth Sci.*, *21*, 157–170, 1984.

Cousens, B. L., R. L. Chase, and J. G. Schilling, Geochemistry and origin of volcanic rocks from Tuzo Wilson and Bowie seamounts, northeast Pacific Ocean, *Can. J. Earth Sci.*, *22*, 1609–1617, 1985.

Cowan, D. S., M. Botros, and H. P. Johnson, Bookshelf tectonics: rotated crustal blocks within the Sovanco fracture zone, *Geophys. Res. Lett.*, *13*, 995–998, 1986.

Davis, E. E., and R. G. Currie, Geophysical observations of the northern Juan de Fuca ridge system: lessons in seafloor spreading, *Can. J. Earth Sci.*, *30*, 278–300, 1993.

Davis, E. E., and R. D. Hyndman, The structure and tectonic history of the northern Cascadia subduction zone: Recent accretion and deformation, *Geol. Soc. Am. Bull.*, *101*, 1465–1480, 1989.

Davis, E. E., and C. R. B. Lister, Tectonic structures on the Juan de Fuca ridge, *Geol. Soc. Am. Bull.*, *88*, 346–363, 1977.

Davis, E. E., and R. P. Riddihough, The Winona Basin: Structure and tectonics, *Can. J. Earth Sci.*, *19*, 767–788, 1982.

Dehler, S. A., and R. M. Clowes, The Queen Charlotte Islands refraction project, part I, The Queen Charlotte fault zone, *Can. J. Earth Sci.*, *25*, 1857–1870, 1988.

DeMets, C., R. G. Gordon, D. F. Argus, and S. Stein, Current plate motions, *Geophys. J. Int.*, *101*, 425–478, 1990.

DeMets, C., R. G. Gordon, D. F. Argus, and S. Stein, Effect of recent revision to the geomagnetic reversal time scale on estimates of current plate motions, *Geophys. Res. Lett.*, *21*, 2191–2194, 1994.

Dewey, J. W., Seismicity and tectonics of western Venezuela, *Bull. Seismol. Soc. Am.*, *62*, 1711–1752, 1972.

Douglas, A., Joint epicentre determination, *Nature*, *215*, 47–48, 1967.

Dragert, H., and R. D. Hyndman, Continuous GPS monitoring of elastic strain in the northern Cascadia subduction zone, *Geophys. Res. Lett.*, *22*, 755–758, 1995.

Dziak, R. P., and C. G. Fox, Juan de Fuca ridge *T*-wave earthquakes August 1991 to present: Volcanic and tectonic implications (abstract), *Eos Trans. AGU*, *76*(46), Fall Meet. Suppl., F410, 1995.

Dziak, R. P., and C. G. Fox, The January 1998 earthquake swarm at Axial Volcano, Juan de Fuca Ridge: Hydroacoustic evidence of a seafloor volcanic activity, *Geophys Res. Lett.*, *26*, 3429–3432, 1999.

Dziak, R. P., C. G. Fox, and A. E. Schreiner, The June–July 1993 seismo-acoustic event at CoAxial segment, Juan de Fuca ridge: Evidence for a lateral dike injection, *Geophys. Res. Lett.*, *22*, 135–138, 1995.

Dziewonski, A. M., G. Ekström, and M. P. Salganik, Centroid-moment tensor solutions for October–December, 1993, *Phys. Earth Planet. Inter.*, *85*, 215–225, 1994.

Engebretson, D. C., A. Cox, and R. G. Gordon, Relative motions between oceanic and continental plates in the Pacific Basin, *Spec. Pap. Geol. Soc. Am.*, *206*, 59 pp., 1985.

Forsyth, D., and S. Uyeda, On the relative importance of the driving forces of plate motion, *Geophys. J. R. Astron. Soc.*, *43*, 163–200, 1975.

Gripp, A. E., and R. G. Gordon, Current plate velocities relative to the hotspots incorporating the NUVEL-1 global plate motion model, *Geophys. Res. Lett.*, *17*, 1109–1112, 1990.

Gutenberg, B., and C. F. Richter, *Seismicity of the Earth and Associated Phenomena*, 2nd ed., Princeton Univ. Press, Princeton, N. J., 1954.

Hanks, T. C., and H. Kanamori, A moment magnitude scale, *J. Geophys. Res.*, *84*, 2348–2350, 1979.

Horn, J. R., R. M. Clowes, R. M. Ellis, and D. N. Bird, The seismic structure across an active oceanic/continental transform fault zone, *J. Geophys. Res.*, *89*, 3107–3120, 1984.

Huang, P. Y., S. C. Solomon, E. A. Bergman, and J. L. Nábělek, Focal depths and mechanisms of Mid-Atlantic Ridge earthquakes from body wave inversion, *J. Geophys. Res.*, *91*, 579–598, 1986.

Hyndman, R. D., and R. M. Ellis, Queen Charlotte fault zone: Microearthquakes from a temporary array of land stations and ocean bottom seismographs, *Can. J. Earth Sci.*, *18*, 776–788, 1981.

Hyndman, R. D., and G. C. Rogers, Seismicity surveys with ocean bottom seismographs off western Canada, *J. Geophys. Res.*, *86*, 3867–3880, 1981.

Hyndman, R. D., and D. H. Weichert, Seismicity and rates of relative motion on the plate boundaries of western North America, *Geophys. J. R. Astron. Soc.*, *73*, 59–82, 1983.

Hyndman, R. D., R. P. Riddihough, and R. Herzer, The Nootka fault zone—A new plate boundary off western Canada, *Geophys. J. R. Astron. Soc.*, *58*, 667–683, 1979.

Hyndman, R. D., T. J. Lewis, J. A. Wright, M. Burgess, D. S. Chapman, and M. Yamano, Queen Charlotte fault zone: Heat flow measurements, *Can. J. Earth Sci.*, *19*, 1657–1669, 1982.

Johnson, H. P., M. A. Hutnak, R. P. Dziak, C. G. Fox, I. Urcuyo, C. Fisher, J. P. Cowen, and J. Nábělek, Earthquake-induced changes in a hydrothermal system at the Endeavour Segment, Juan de Fuca Ridge, *Nature*, *407*, 174–177, 2000.

Karsten, J. L., S. R. Hammond, E. E. Davis, and R. G. Currie, Detailed geomorphology and neotectonics of the Endeavor segment, Juan de Fuca ridge: New results from SeaBeam swath mapping, *Geol. Soc. Am. Bull.*, *97*, 213–221, 1986.

Kreemer, C., R. Govers, K. P. Furlong, and W. E. Holt, Plate boundary deformation between the Pacific and North America in the Explorer region, *Tectonophysics*, *293*, 225–238, 1998.

Kulm, L. D., R. von Huene, J. R. Duncan, J. C. Ingle, S. A. Kling, L. F. Musich, D. J. W. Piper, R. M. Pratt, H.-J. Schrader, O. Weser, and S. W. Wise Jr., Site 177, *Initial Rep. Deep Sea Drill. Proj.*, *18*, 233–285, 1973.

Lewis, T. J., C. Lowe, and T. S. Hamilton, The continental signature of a ridge-trench-transform triple junction: northern Vancouver Island, *J. Geophys. Res.*, *102*, 7767–7781, 1997.

Lister, C. R. B., Plate tectonics at an awkward junction: Rules for the evolution of Sovanco Ridge area, *NE Pacific, Geophys. J.*, *96*, 191–201, 1989.

Lonsdale, P., Structural patterns of the Pacific floor offshore of Peninsular California, in *Gulf and Peninsular Province of the Californias*, edited by J. P. Dauphin and B. R. T. Simoneit, *AAPG Mem.*, *47*, 87–143, 1991.

Mackie, D. J., R. M. Clowes, S. A. Dehler, R. M. Ellis, and L. P. Morel-A-L'Huissier, The Queen Charlotte Islands refraction project, part II, Structural model for transition from Pacific to North America plate, *Can. J. Earth Sci.*, *26*, 1713–1725, 1989.

Michael, P. J., R. L. Chase, and J. F. Allan, Petrologic and geologic variations along southern Explorer Ridge, northeast Pacific Ocean, *J. Geophys. Res.*, *94*, 13,895–13,918, 1989.

Nábělek, J., and G. Xia, Moment-tensor analysis using regional data: application to the 25 March, 1993, Scotts Mills, Oregon earthquake, *Geophys. Res. Lett.*, *22*, 13–16, 1995.

Nicholson, C., C. C. Sorlien, T. Atwater, J. C. Crowell, and B. P. Luyendyk, Microplate capture, rotation of the western Transverse Ranges, and initiation of the San Andreas transform as a low-angle fault system, *Geology*, *22*, 491–495, 1994.

Riddihough, R. P., A model for recent plate interactions off Canada's west coast, *Can. J. Earth Sci.*, *14*, 384–396, 1977.

Riddihough, R. P., Gorda plate motions from magnetic anomaly analysis, *Earth Planet. Sci. Lett.*, *51*, 163–170, 1980.

Riddihough, R. P., Contemporary movements and tectonics on Canada's west coast: A discussion, *Tectonophysics*, *86*, 319–341, 1982.

Riddihough, R. P., Recent movements of the Juan de Fuca plate system, *J. Geophys. Res.*, *89*, 6980–6994, 1984.

Riddihough, R. P., R. G. Currie, and R. D. Hyndman, The Dellwood Knolls and their role in triple junction tectonics off northern Vancouver Island, *Can. J. Earth Sci.*, *17*, 577–593, 1980.

Rohr, K. M. M., and J. R. Dietrich, Strike slip tectonics and development of the Tertiary Queen Charlotte Basin, offshore western Canada: Evidence from seismic reflection data, *Basin Res.*, *4*, 1–19, 1992.

Rohr, K. M. M., and K. P. Furlong, Ephemeral plate tectonics at the Queen Charlotte triple junction, *Geology*, *23*, 1035–1038, 1995.

Rohr, K. M. M., M. Scheidhauer, and A. M. Trehu, Transpression between two warm mafic plates: The Queen Charlotte Fault revisited, *J. Geophys. Res.*, *105*, 8147–8172, 2000.

Scheidhauer, M., Crustal structure of the Queen Charlotte transform fault zone from multichannel seismic reflection and gravity data, M.Sc. thesis, 184 pp., Oreg. State Univ., Corvallis, 1997.

Spindler, C., G. C. Rogers, and J. F. Cassidy, The 1978 Brooks peninsula, Vancouver Island, earthquakes, *Bull. Seismol. Soc. Am.*, *87*, 1011–1023, 1997.

Srivastava, S. P., D. L. Barrett, C. E. Keen, K. S. Manchester, K. G. Shih, D. L. Tiffin, R. L. Chase, A. G. Thomlinson, E. E. Davis, and C. R. B.

Lister, Preliminary analysis of geophysical measurements north of Juan de Fuca ridge, *Can. J. Earth Sci.*, *8*, 1265–1281, 1971.

Stock, J. M., and J. Lee, Do microplates in subduction zones leave a geologic record?, *Tectonics*, *13*, 1472–1487, 1994.

Stock, J. M., and P. Molnar, Uncertainties and implications of the Cretaceous and Tertiary position of North America relative to Farallon, Kula, and Pacific plates, *Tectonics*, *6*, 1339–1384, 1988.

Sweeney, J. F., and D. A. Seemann, Crustal density structure of Queen Charlotte Islands and Hecate Strait, British Columbia, in *Evolution and Hydrocarbon Potential of the Queen Charlotte Basin, British Columbia*, edited by G. Woodsworth, *Pap. Geol. Surv. Can.*, *90-10*, 89–96, 1991.

Tiffin, D. L., B. E. B. Cameron, and J. W. Murray, Tectonics and depositional history of the continental margin off Vancouver Island, British Columbia, *Can. J. Earth Sci.*, *9*, 280–296, 1972.

Turcotte, D. L., and G. Schubert, *Geodynamics: Applications of Continuum Physics to Geological Problems*, John Wiley, New York, 1982.

Wahlström, R., and G. C. Rogers, Relocation of earthquakes west of Vancouver Island, British Columbia, 1965–1983, *Can. J. Earth Sci.*, *29*, 953–961, 1992.

Wahlström, R., G. C. Rogers, and R. E. Baldwin, *P*-nodal focal mechanisms for large earthquakes offshore Vancouver Island, *Geol. Surv. Can. Open File Rep., 2268*, 1990.

Wessel, P., and W. H. F. Smith, New version of the generic mapping tools released, *Eos Trans. AGU*, *76*, 329, 1995.

Wilson, D. S., A kinematic model for the Gorda deformation zone as a diffuse southern boundary of the Juan de Fuca plate, *J. Geophys. Res.*, *91*, 10,259–10,269, 1986.

Wilson, D. S., Deformation of the so-called Gorda plate, *J. Geophys. Res.*, *94*, 3065–3075, 1989.

Wilson, D. S., Confidence intervals for motion and deformation of the Juan de Fuca plate, *J. Geophys. Res.*, *98*, 16,053–16,071, 1993.

Yorath, C. J., and R. D. Hyndman, Subsidence and thermal history of Queen Charlotte Basin, *Can. J. Earth Sci.*, *20*, 135–159, 1983.

Yuan, T., G. D. Spence, and R. D. Hyndman, Structure beneath Queen Charlotte Sound from seismic-refraction and gravity interpretation, *Can. J. Earth Sci.*, *29*, 1509–1529, 1992.

J. Braunmiller, Swiss Seismological Service, ETH-Hönggerberg, CH-8093 Zurich, Switzerland. (jochen@seismo.ifg.ethz.ch)

J. Nábělek, College of Oceanic and Atmospheric Sciences, Oregon State University, Corvallis, OR 97331, USA. (nabelek@oce.orst.edu)